

Could the Lunar ‘Late Heavy Bombardment’ Have Been Triggered by the Formation of Uranus and Neptune?

Harold F. Levison

Luke Dones

Clark R. Chapman

S. Alan Stern

Space Studies Department

Southwest Research Institute, Boulder, CO 80302

Martin J. Duncan

Department of Physics, Queen’s University

Kingston, Ontario, Canada K7L 3N6

and

Kevin Zahnle

NASA Ames Research Center

MS 245-3, Moffett Field, CA 94035

To appear in *Icarus*

Abstract

We investigate the hypothesis that the so-called Late Heavy Bombardment (LHB) of the Moon was triggered by the formation of Uranus and Neptune. As Uranus and Neptune formed, which we assume occurred at the epoch of the LHB, they scattered neighboring icy planetesimals throughout the Solar System. Some of these objects hit the Moon. Our integrations show that the Moon would have accreted about 6×10^{21} g, if we assume that the Uranus-Neptune region initially contained 5 times the current mass of these planets in the form of small solid objects. In addition, Mars would have accumulated $\sim 6 \times 10^{22}$ g of icy material, which could have supplied its putative early massive atmosphere. However, Earth would likely have accreted only $\sim 7 \times 10^{22}$ g of water, or $\sim 5\%$ of its oceans, through the mechanisms studied here. The numerical experiment that we have performed on the behavior of Uranus-Neptune planetesimals shows very good agreement with current constraints on the LHB. The influx of Uranus-Neptune planetesimals onto the Moon could have lasted for a time as short as 10 or 20 million years. The dynamical transport of the Uranus-Neptune planetesimals during this process would have caused Jupiter and Saturn to migrate. This migration, in turn, would have destabilized objects in the Jovian Trojan swarms and the asteroid belt. Thus, not only would Uranus and Neptune planetesimals have struck the Moon, but asteroids would have as well. We find that the Trojan asteroids of Jupiter could not have contributed a large percentage of material to the LHB, but the asteroid belt could, in principle, have contributed to, or even dominated, the LHB. Although this model appears to explain the LHB well, it requires that fully formed Uranus and Neptune not appear in the trans-saturnian region until some 700 million years after the formation of the Earth.

I. Introduction

The ‘Late Heavy Bombardment’ (hereafter LHB) was a phase in the impact history of the Moon that occurred roughly 4.0 to 3.8 Gyr ago. It was during the LHB that the lunar basins with known dates were formed. The LHB was either the tail-end of accretion or it may have been a spike in the impact rate (‘terminal cataclysm,’ Tera et al. 1974) at that time. In either case, it marks the final epoch when the dominant surface geology of the Moon was created by large impacts; afterwards, mare volcanism dominated for a while, and the subsequent production of larger craters from the end of the LHB to the present time is highly undersaturated.

It is often assumed that the LHB created the heavily cratered terrains on other planets and satellites as well as on the Moon (Neukum 1983). If it was indeed widespread, the LHB provides a marker horizon in the chronology of the Solar System. Certainly, the end of the LHB marks the beginning of the epoch when the sustained origins of life became possible on the Earth following possible ‘frustration’ by impacts (e.g. Maher & Stevenson 1988; Sleep et al. 1989; Oberbeck & Fogleman 1989; see Ryder 2000 for a contrary view of impact frustration). The LHB may even have contributed a major portion of the volatiles (especially complex organics) necessary for the origin and sustenance of life (Chyba 1991). Prior to the end of the LHB, the Moon’s surface was significantly altered by crater- and basin-forming impacts. But it remains controversial (Hartmann et al. 2000) whether *i*) these impacts occurred over hundreds of millions of years (from 4.3 to 3.8 Gyr; Baldwin 1987a,b, Neukum 1977) or, instead, *ii*) there was a spike in the impact flux, lasting tens of millions of years (at 3.9–3.8 Ga) during which seven or more basin-forming events occurred (Dalrymple & Ryder 1993; see §II for a more complete discussion). Following the decline in bombardment rate, the crusts and surfaces of the different bodies could develop and follow separate evolutionary tracks determined mainly by internal processes.

The LHB was discovered in the late 1960s, though it was actually proposed by Baldwin (1949) before Apollo dating of lunar rocks conclusively demonstrated it. It is characterized by the impact of at least a few $\times 10^{21}$ g of material onto the Moon (see §II) followed by a precipitous decline in the lunar bombardment rate subsequent to ~ 3.85 Ga. Tera et al. (1974), interpreting a peak in isotopic recrystallization ages of lunar rocks, invoked the variant on the LHB termed the ‘lunar cataclysm,’ in which there was a sudden increase followed by a sudden decrease in the bombardment rate (duration $\lesssim 100$ Myr), compared with preceding and following epochs. Hartmann (1975) called the cataclysm a ‘misconception’ and argued that an inevitable ‘stone-wall’ effect reflected what was actually a monotonically decaying cratering flux (Grinspoon 1989, see also Hartmann et al. 2000). Later, Hartmann (1980) adopted a composite picture of lunar impact history, with episodic spikes (perhaps with one corresponding to the cataclysm) superimposed on an exponential decay from accretionary epochs.

Independent of the form of the LHB (i.e. cataclysm or not), there remains no generally accepted explanation for the bombardment. The LHB might simply represent the late accretion of planetesimals and debris left over from the formation of the terrestrial planets (Morbidelli et al. 2001), although it seems likely that the timescales for the clearing of these objects were short compared to the ~ 700 Myr from Solar System origin until the LHB. Another theory (Wetherill 1975) ties the LHB to the formation of Uranus and Neptune, which likely were the last planets to accrete and which could have altered the dynamical state of the planetary system for more than a half billion years after the formation of the terrestrial planets.

Still other models (Chapman & Davis 1975; Chapman 1976; Zappalà et al. 1998) associate the LHB with collisional processes in the early asteroid belt. Zappalà et al. (1998) showed that ‘family forming event[s]’ (i.e. collisions between two large asteroids) near various main-belt mean-motion resonances can produce

asteroid showers lasting from 5 to 80 Myr. Such asteroid showers are plausible sources for the LHB impactors. In this model, the mass required in the belt to explain the amount of mass accreted by the Moon is $\sim 3 \times 10^{24}$ g for a source in the innermost belt, 5×10^{25} g for a source near the 3:1 resonance, and $\sim 10^{27}$ g for an outer-belt source. These mass requirements reflect the relative unlikelihood of any given asteroid striking the Moon, and the demand that the Moon accreted a least a few $\times 10^{21}$ g. (In addition, they were calculated assuming that all the collisional fragments are injected into a resonance, which is unlikely.) The inner belt mass required is comparable to the mass of the entire present-day belt, but is almost 1000 times larger than the mass of the largest asteroid today with $a < 2.3$ AU. The main problem with this model is that collisional disruption of the required Ceres-sized asteroid is very improbable, unless the mass of the belt at 3.9 Ga was still of order $1M_{\oplus}$. If the asteroid belt were really this massive, neglecting collective gravitational interactions between asteroids is probably not valid. In particular, such a massive belt might stop members in resonances from reaching large eccentricities (Ward & Hahn 1998b) and being delivered to the Moon (see §III for a more complete discussion).

Finally, one concept (Ryder 1990, although see Section 5 of Hartmann et al. 2000) views the LHB as specific to the Earth-Moon system and a natural outgrowth of the formation of the Moon itself. Conceivably, there are other potential long-term reservoirs (e.g., Trojans of various planets) for material that could suddenly be released, by collisional or dynamical processes, long after primary accretion was finished in the inner Solar System.

This is the first in a series of papers in which we investigate the dynamics of potential impactors under each of the above scenarios by applying modern numerical methods for, in many cases, the first time. Our purpose is not to advocate one model over another, because we feel that constraints, such as the lunar cratering record

and the chronology of planet formation, are not yet well enough known. Instead, we intend to supply detailed dynamical information that may help future researchers decide between the available scenarios.

In this paper we investigate Wetherill's 1975 suggestion that the LHB resulted from the formation of Uranus and Neptune. Before we discuss our results, we first address two arguments against the idea that the LHB impactors originated in the outer solar system. If either of these arguments are true then the models presented in this paper are most likely not.

Strom & Neukum (1988) inferred from the crater size distributions on Mercury, the Moon, and Mars that the semi-major axes of the LHB impactors must lie between 0.8 and 1.2 AU. This result follows from the assumption that the differences seen between the crater size distributions on these three worlds were the result of different impact velocities. However, the crater morphologies on Mars have been shaped by grossly different processes that have not operated on the Moon and Mercury. Also Strom & Neukum (1988) only consider crater diameters near the transition between complex craters and multi-ring craters where the crater diameter is difficult to determine. Thus, we believe that the observed shifts in the cratering curves between different worlds are likely to be the result of geological processes rather than the result from differences in impact velocities.

Recently, Swindle & Kring (2001) have argued that the LHB impactors could not have been cometary because such a source would have delivered orders of magnitude more argon to Earth than is currently observed. This argument is based on an extrapolation of the detected argon abundance in comet Hale-Bopp (Stern et al. 2001) to the entire LHB. However, there are several uncertainties to this argument. First, Stern et al. measured the abundance of argon to oxygen in Hale-Bopp's coma. It is not fully clear how this relates to the overall abundance ratio because oxygen and argon most likely are coming from different depths within

the comet. Second, Swindle & Kring (2001)'s argument assumes that Hale-Bopp has the same chemical composition as the typical LHB impactor. Recent dynamical models (Levison et al. 1999) show that a significant fraction of the Oort cloud may have originated in the Kuiper belt. These objects, of which Hale-Bopp may be a member, formed at greater heliocentric distance than our suggested LHB impactors (which come from between Uranus and Neptune), and thus may have formed with significantly more argon. Finally, Swindle & Kring assume that LHB impactors will retain their argon as they evolve through the inner solar system on their way to the Earth. However, Jupiter-family comets, which are dynamically similar to our proposed LHB impactors, spend roughly 7000 years on orbits that bring them close to the Sun (Levison et al. 2000), thus it seems likely that most of the argon will be lost as the impactor heats while in similar orbits.

Thus, we do not believe that there is a strong argument that can rule out the Uranus-Neptune region as the source of the LHB and that this scenario should be modeled. We base our simulations on Fernández & Ip (1984)'s models of the formation of Uranus and Neptune, the details of which are presented in §III. Before we discuss these models, however, in §II we discuss the current constraints on the impact flux on the Moon during the LHB. In §IV and §V we present the initial conditions and the results of our dynamical simulations, respectively. In §VI we present our concluding remarks.

II. The Early Impact Record of the Moon

In this section, we review observational constraints on the Late Heavy Bombardment in order to estimate the amount of mass that has impacted the Moon and when these impacts took place.

Although no direct record of early impacts remains on the Earth, the lunar record is better preserved (Sleep et al. 1989; Chyba 1991; Zahnle & Sleep 1997; Hartmann et al. 2000; Ryder et al. 2000; Mojzsis & Ryder 2000). We consider three arguments that constrain the mass of material impacting the Moon between the solidification of the lunar crust some 4.4 Gyr ago (Carlson & Lugmair 1979, 1988) and the end of the LHB about 3.8 Gyr ago. (1) The contamination of the lunar crust with meteoritic material provides an estimate of the total mass *accreted* by the Moon since the lunar crust formed. (2) Counts of primary craters on dated lunar surfaces constrain the number of impactors on the Moon. The energies released by basin-forming impacts can be estimated, yielding, for assumed asteroidal or cometary impact velocities, the masses of the impactors. (3) Impact stirring has been mild enough that (a) the lunar crust remains heterogeneous and (b) the lunar mantle has seldom been excavated. We now briefly review each of these lines of evidence.

(1) Crustal Contamination. The mantle and crust of Earth are highly depleted in siderophile elements such as Ir, which enter the metallic iron core in preference to silicate phases. The lunar mantle is even more depleted in siderophiles than the Earth (Sleep et al. 1989). The presence of Ir in the lunar crust is thus likely due to meteoritic contamination, and crustal siderophile abundances have long been used in attempts to constrain the bombardment history of the Moon (Morgan et al. 1977). However, estimates of the total mass accreted by the Moon since its crust solidified, M_A , have ranged over two orders of magnitude, from $> 5 \times 10^{23}$ g (Hartmann 1980) to 8×10^{22} g (Sleep et al. 1989) down to 5×10^{21} g (Ryder 1999; Ryder's Table

1 summarizes these determinations). These estimates differ in their assumptions about the mass fraction of the lunar crust that is of meteoritic origin, f , and the thickness of crust that is contaminated, T . For instance, Sleep et al. (1989) assume $f = 2\%$ and $T = 35$ km, while Ryder (1999) assumes $f = 0.3\%$ and $T = 15$ km.

A more fundamental uncertainty is that the fraction of the impactor's mass *retained* after an impact depends upon the impactor's orbit. Not all material colliding with the Moon is retained, since if the impact velocity is high enough, much of the impactor escapes to space. The mass *incident* on the Moon, M , thus could be substantially greater than the mass accreted by the Moon. We can write $M_A = \eta M$, where the retention efficiency $\eta \leq 1$, and may be $\ll 1$. Chyba (1991) argued that $\eta \sim 1/2$. In our simulations (§V) we find a typical lunar impact speed for Uranus-Neptune planetesimals of 16 km/s, somewhat higher than the 12 km/s used by Chyba, based upon data for known Earth-crossing asteroids. Furthermore, recent simulations find that little of the impactor is accreted in the half of all impacts that occur at angles $\geq 45^\circ$ to the normal, even at low speeds (Pierazzo & Melosh 2000a,b). Both factors argue that η is likely to be considerably less than 1/2. We will take $\eta = 1/10$, but this value is open to debate. Crustal contamination thus provides only an uncertain lower limit on the mass impacting the Moon. This lower limit is $M = M_A/\eta = 8 \times 10^{22} \text{ g}/(1/10) \sim 8 \times 10^{23} \text{ g}$ for Sleep et al. (1989)'s value of M_A , and $5 \times 10^{22} \text{ g}$ for Ryder's. We emphasize that this constraint refers to the *entire* history of the Moon since it solidified, so the impacting mass is expected to be greater than the value we infer below for the LHB.

(2) *Craters and Basins.* The dated lunar maria, which have an average age of 3.25–3.65 Gyr, are sparsely cratered, compared with the lunar highlands, which are at most about 1 Gyr older (Hartmann et al. 1981, Table 8.4.2 and Figure 8.4.1). Hartmann et al. (2000) therefore estimate that the cratering rate for the first billion years of lunar history must have averaged at least ~ 100 times higher

than the rate since then. Debate still rages about whether the impact rate on the Moon has declined more-or-less monotonically with time, or whether there was a period of relative calm prior to an ‘impact cataclysm’ that resulted in the formation of the well-known nearside basins such as Imbrium and Orientale at ~ 3.8 – 3.9 Ga (Hartmann et al. 2000).

Wilhelms (1987, pp. 64–65) lists 28 ‘definite’ and 17 ‘probable [or] possible’ lunar basins, which he defines as craters with diameters $D \geq 300$ km. South Pole-Aitken ($D = 2500$ km) is generally taken to be the largest lunar basin^[1]. Zahnle & Sleep (1997) estimate the energy of the South Pole-Aitken impactor as $\sim 10^{34}$ ergs, give or take a factor of 4. This corresponds to an impactor mass of $8\frac{\times}{\div}4 \times 10^{21}$ g at an assumed impact speed $v = 16$ km/s. South Pole-Aitken predates the other confirmed lunar basins, but its formation time is unknown.

In terms of the volume excavated during the impact, the South Pole-Aitken event was some 5–6 times larger than each of the impacts that formed the next three largest known lunar basins – Imbrium ($D = 1160$ km), Serenitatis (740 km), and Crisium (1060 km) (Wieczorek & Phillips 1999). Serenitatis and Crisium belong to the ‘Nectarian’ system, which includes 11 or 12 basins that formed in a period that began with the formation of the Nectaris basin (860 km) and ended just prior to the formation of the Imbrium basin (Wilhelms 1987, Table 9.3). The Apollo 14/15, 16, and 17 landing sites appear to be dominated by ejecta from the formation of Imbrium, Nectaris, and Serenitatis, respectively (Wetherill et al. 1981, pp. 971–974).

Imbrium appears much ‘fresher’ than Serenitatis and Nectaris (e.g., Wilhelms 1987, p. 173), and the Apollo 14 and 15 landing sites, which are dominated by Imbrium ejecta, have fewer superposed craters. It was thus anticipated prior to

[1] The existence of Procellarum ($D = 3200$ km), the largest ‘possible’ basin, remains questionable (Smith et al. 1997).

the Apollo landings that Imbrium formed much later. Instead, dated lunar samples suggest that the Imbrium basin formed only some 70 Myr after Nectaris: in the chronology of Wilhelms (1987; also see Hartmann et al. 2000, Figure 6), Nectaris formed at 3.92 Ga, while Imbrium formed at 3.85 Ga.

The date of Imbrium is more secure than the age of Nectaris (Hartmann et al. 2000). Soil samples taken from the Apollo 16 site fell into three age groups: ~ 4.1 Ga; ~ 3.9 Ga; and < 2.5 Ga (Wetherill et al. 1981, Taylor 1982, pp. 238-241, Nyquist & Shih 1992). The intermediate age group contained one totally melted KREEP basalt, suggesting a deep impact, and has been taken by most researchers to date the formation of the Nectaris basin. However, some favor a 4.1 Gyr age for Nectaris (Wetherill 1981; Neukum & Ivanov 1994). A date for Nectaris near 3.9 Ga strongly suggests that a cataclysm took place, while a 4.1 Ga date is more consistent with a smoothly declining impact flux (Hartmann et al. 2000).

Assuming an Imbrium impact energy of $(2 \pm 1) \times 10^{33}$ ergs (Zahnle and Sleep 1997), and again assuming $v = 16$ km/s, we estimate the mass of the Imbrium impactor to be 2×10^{21} g, and the total mass of the impactors that produced the Nectarian basins to be $\sim 4 \times 10^{21}$ g. Thus a total of some 6×10^{21} g struck the Moon during some 50 Myr (Ryder’s chronology), 70 Myr (Wilhelms), or 200 Myr (Neukum & Ivanov)^[2]. This mass estimate is uncertain by at least a factor of two up or down, due to uncertainties in the energy of the Imbrium impact, the

[2] We assumed that the mass distribution of the impactors was relatively flat (*i.e.*, top-heavy) up to the masses of the basin forming impactors, and then steepened at larger masses. In this case most of the mass is near the ‘knee’ of the distribution. Our assumption is motivated by the observed size distribution of the late basins and the lack of larger, mantle-excavating impacts (see argument 3(b) in this section). Thus we essentially assume that the largest ‘potential impactor’ for the Moon and the terrestrial planets was about the same size. In this case most of the mass was in the impactors that formed the basins, so that we could just add up the masses of the impactors that made the

speeds of the impactors, and the crater scaling relation. For our purposes, the main point is that at least 12 basins with diameters greater than 300 km formed around 3.9–3.8 Ga – i.e., some 500–600 Myr after the lunar crust solidified. For our assumed crater scaling relation, this implies that at least 12 bodies with masses greater than $(2 \pm 1) \times 10^{19}$ g, and at least 2 bodies with masses greater than $(1.0 \pm 0.5) \times 10^{21}$ g, struck the Moon during this period. For impactor densities between 1 and 2 g/cm³, these impactor masses correspond to impactor diameters of 22–39 km for 300 km basins, and to impactor diameters of 77–141 km for 1000 km basins. Presumably dozens of 10^{21} g bodies would have struck the Earth, with its much larger cross-section ($\gtrsim 13\times$). Thus a large number of ~ 100 km bodies must have been ‘stored’ for half a billion years. (For comparison, at present there are only about 200 asteroids bigger than 100 km in the entire main asteroid belt (Cellino et al. 1991), while the Kuiper Belt and ‘scattered disk’ beyond Neptune each appears to contain tens of thousands of 100 km bodies (Trujillo et al. 2000).) This storage problem has long been recognized (Wetherill 1975).

The cratering rate appears to have declined to approximately its present rate soon after the formation of the late nearside basins. Wilhelms (1987, Table 11.1, p. 230) finds that the cratering rate declined rapidly between 3.72 Ga and 3.57 Ga and then leveled off. Only one basin, Orientale (930 km), is known to have formed after Imbrium, at ~ 3.8 Ga. The largest crater known to have formed during the Eratosthenian period, i.e., the last 3.2 Gyr, is Langrenus, which is only 132 km in diameter (McEwen et al. 1993, Dones et al. 2001).

(3) *Impact Stirring.* There are two arguments related to lunar geology that suggest a modest rate of basin formation subsequent to the solidification of the lunar crust and the epoch of the LHB about 0.5 Gyr later.

(a) *Possibly Undersaturated Basin Record.* If there were as much as 8×10^{22} g of

Nectarian basins and Imbrium to infer the total mass that struck the Moon during the LHB.

accreted mass, as inferred by Sleep et al. (1989), a minimum of ~ 40 Imbrium-scale impact craters would have formed on the lunar surface, and more if $\eta < 1$. In fact, there are only about 9 such basins with area larger than about half the area of Imbrium, including Imbrium itself, totaling just 22% of the surface area of the Moon. Possibly these are most of the large basins that ever formed, in which case the fact that the first 5 took about 0.5 Gyr to form and the last 4 only 70 Myr indicates a powerful spike in basin-forming rate during the LHB. On the other hand, empirical saturation equilibrium (Hartmann 1984) is near 25% surface area coverage, at least for smaller craters. So it is possible that the observed basins represent just the more recent impacts rather than the totality of basin impacts. Whether earlier basins could have been destroyed by subsequent cratering and basin formation depends on two uncertain and controversial issues: (i) the efficacy of ejecta blankets and basin secondaries in destroying pre-existing topography and (ii) the degree to which such large topographic features relax to the point of disappearance with age.

(b) *Minimum Mantle Penetration.* A stronger argument that pre-Nectarian basin formation was modest is the minimal evidence that the lunar mantle was excavated. (The South Pole-Aitken impactor came close but probably did not do so (Pieters et al. 1997) although the smaller Crisium impact may have done so [Wieczorek & Phillips 1998].) If the impactor mass distribution remained flat (i.e. top-heavy) for masses about 10^{21} g, as has sometimes been assumed (e.g. Chyba 1991, Zahnle & Sleep 1997), numerous additional impactors beyond those represented by observable basins would likely have been accompanied by impactors much larger than the Imbrium impactor and would likely have excavated lunar mantle materials. However, troctolite, an expected constituent of the lower crust which was excavated by Imbrium, is rare (Marvin et al. 1989). So it is likely that most of the post-crustal impact basins ever formed are still visible and that Nectarian-aged basins represent a true spike in the early impact history of the Moon.

As many authors have pointed out, the Apollo and Luna landing sites lie within a small area of the lunar nearside, so the interpretation of rock ages is complicated by issues such as possible contamination by Imbrium ejecta (Haskin et al. 1998, although see Ryder et al. 2000 and Hartmann et al. 2000). Cohen et al. (2000) argue on the basis of the dating of a small number of lunar meteorites, which apparently came from a wide variety of locations, that a spike in the lunar impact record did indeed occur. Radiometric dating of a wide variety of sites on the Moon, either by studying lunar spherules (similar to Culler et al. 2000), further lunar meteorites or samples from future spacecraft return missions, should resolve whether a cataclysm took place.

In summary, based upon the above discussion, we will make two assumptions for our comparison with numerical experiments below. They are: (1) The late lunar basins (e.g., Nectaris and Imbrium) formed during a period lasting some 100 Myr. (2) Approximately 6×10^{21} g of material hit the Moon during this period. While these assumptions are *consistent* with an impact cataclysm, we do not assert that a cataclysm necessarily occurred. Rather, our goal is to construct a plausible dynamical model of a cataclysm.

III. Assumed Model for the Formation of Uranus and Neptune

The chronology of the formation of the planets is not well understood, particularly for the outer planets. However, a few facts are clear. Owing to their near solar composition, Jupiter and Saturn must have formed before the solar nebula dispersed (in $\sim 10^6$ to 10^7 years), although it has been difficult to construct models that can form their solid cores on this timescale (see Pollack et al. 1996; but see Boss 1997 for another perspective). Jupiter and Saturn formed as the terrestrial planets started to accumulate, but must have finished forming before the terrestrial planets. Radioisotope data and models of the late stages of terrestrial planet formation put the final accumulation of the terrestrial planets at about $\sim 10^8$ years (Halliday et al. 2000; Chambers & Wetherill 1998; Agnor et al. 1999). However, these models should be viewed with some suspicion since they overestimate the eccentricities and spin rates for the terrestrial planets (Agnor et al. 1999).

The situation for Uranus and Neptune is even less clear. Monte Carlo models by Fernández & Ip (1984) put the late stages of formation at $\sim 10^8$ years. However, an attempt to reproduce these results by Lissauer et al. (1995) using similar methods failed. Stewart & Levison (1998) attempted to form Uranus and Neptune using direct orbital integrations and Fernández & Ip's initial conditions. They also failed to form these planets. Brunini & Fernández (1999) recently reported a success using direct integrations, but they now acknowledge problems with their published integrations and now agree with the Stewart & Levison results (A. Brunini, pers. communication). Thus, currently the standard model for the formation of Uranus and Neptune does not appear to work.

It appears that Uranus and Neptune fail to form at all, given the physical assumptions in Fernández & Ip's 1984 paper. This is because the protoplanetary embryos dynamically excite each other to large relative velocities, increasing the

volume of space that they occupy. This decreases the collision rate to very low values and Uranus and Neptune-like planets do not accrete. Clearly, one or more physical processes are missing from these simulations and more sophisticated models are needed. At this time, no information exists that significantly constrains the date of the formation of Uranus or Neptune.

Once Uranus and Neptune formed, the orbital evolution of the outer Solar System is better understood. Planet formation is not expected to be 100% efficient. As the masses of Uranus and Neptune approached their full adult values, they must have gravitationally scattered most of the remaining nearby planetesimals both outward into the trans-Neptunian region and inward toward Jupiter and Saturn. Usually the objects scattered outward returned to the Uranus-Neptune region in the next orbit to be scattered again (either inward or outward). Jupiter and Saturn are so massive, however, that they can efficiently eject many of these planetesimals out of the planetary system. Thus, objects scattered outward usually return to Uranus and Neptune, while those scattered inward are effectively removed, thereby causing a net flux of objects toward Jupiter. This inward transport of mass required an outward migration of the orbits of Uranus and Neptune in order to conserve the angular momentum and energy of the system (Fernández & Ip 1984, Hahn & Malhotra 1999). For the same reason, Jupiter migrated inward. Fernández & Ip (1984) found that the migration timescale was between $\sim 10^7$ years and $\sim 10^8$ years.

There may be observational evidence for such a migration in the dynamical structure of the Kuiper belt (Malhotra 1995, 2001). From numerical simulations of the excitation of inclinations of Kuiper belt objects by sweeping mean-motion and secular resonances, Malhotra (1998) argues that the migration timescale must have been ~ 30 Myr. However, these models should be viewed with some skepticism since they assume that both 1) the Kuiper belt was dynamically cold at the beginning

of migration, and 2) the migration was very smooth. Both assumptions are most likely incorrect.

Perhaps a more direct argument for the early migration of the outer planets is the very existence of the Oort cloud. Oort cloud comets are believed to have originated between the giant planets and then been scattered outward during the late stages of planet formation (see Duncan et al. 1987 and Dones *et al.* 2000). Indeed, these are the objects that were responsible for the migration of the giant planets. Weissman (1996) estimates that the original mass of the Oort cloud was of order $10\text{--}100M_{\oplus}$. Hahn & Malhotra (1999) show that constructing such a massive Oort cloud from material between the giant planets requires that Neptune migrate several AU.

If the clearing of planetesimals in the Uranus-Neptune region was indeed responsible for the LHB, then this clearing must have occurred ~ 3.8 Gyr ago – some 700 million years after the formation of the terrestrial planets. As discussed above, this date is not ruled out by current observational or theoretical constraints on the formation of Uranus and Neptune. There are several mechanisms that could have been responsible for this delay: *i*) Uranus and Neptune could have taken this long to form. If the LHB lasted only a few tens of millions of years, Uranus and Neptune must have quickly grown from a mass at which they could not have scattered many of their nearby planetesimals ($\lesssim 10\%$ of their current masses) to the point at which they were very effective at scattering the nearby objects ($\sim 50\%$ of their current masses). This phase could be a manifestation of the transition from runaway growth to the final violent stages of planet formation. *ii*) Uranus and Neptune could have formed earlier, but some mechanism, such as collisions (Stern & Weissman 2000) or collective effects in the nearby planetesimal disk (Ward & Hahn 1998b), could have stopped them from clearing the nearby region. As conditions within the disk changed (for example, the optical depth decreased, and random velocities increased

as objects accreted) these effects would have diminished. *iii*) Uranus and Neptune could have formed much closer to the Sun than normally assumed, near (Stewart & Levison 1998) or inside of the orbit of Saturn (Thommes et al. 1999), and then been gravitationally scattered outward to near their pre-migrated orbits. After this, a massive proto-planetary disk could have circularized their orbits (Thommes et al. 1999). The event that scattered Uranus and Neptune outward would then have indirectly caused the LHB. Such a scenario is not impossible, given that it has been recently shown that hypothetical planetary systems much more compact than our own can be stable for nearly a billion years and then undergo gross orbital changes (Levison et al. 1998).

Given the lack of constraints, the possibilities concerning the formation of Uranus and Neptune are almost endless. So, in order to evaluate the dynamics of the hypothesis that Uranus and Neptune triggered the LHB (as suggested by Wetherill 1975), for the remainder of this paper we will adopt the following simple scenario for the formation of the planets: The terrestrial planets, Jupiter, and Saturn formed approximately 4.5 Gyr ago. The terrestrial planets were in their current orbits, but the orbit of Jupiter was slightly larger than it is now, and the orbit of Saturn was slightly smaller. At this time the proto-planetary particulate disk had an inner edge at ~ 10 AU. This structure remained fixed until the time of the LHB, at which time Uranus and Neptune formed. We assume that they formed at about the same time and did not start clearing out the planetesimal swarm in which they were embedded until they reached close to their current masses.

A note concerning our assumptions: We use the duration of the impactor flux on the Moon as a test of our models for the LHB. However, our assumption that the Uranus-Neptune region very quickly transitioned from a quiescent region to a violent one will minimize the length of time it took them to clear this region. It is likely that the timescales quoted below for the LHB would be lengthened if this

transition occurred more slowly.

For most of our integrations, we adopted as a straw-man a migration scenario similar to that of Malhotra (1995) to study the structure of the Kuiper Belt. In this scenario Jupiter was slightly further from the Sun than it is currently, while the other giant planets were initially closer to the Sun. Following Malhotra (1995), we forced the planets to migrate to their current locations by adding a fictitious acceleration to their orbital integrations. This fictitious force decreased exponentially over time with a time constant of τ . For each set of initial conditions, we performed two simulations, one with $\tau = 10^7$ years and the other with $\tau = 3 \times 10^7$ years, which is consistent with timescales derived from direct numerical integrations of the migration process (Hahn & Malhotra 1999).

The initial positions and velocities for the giant planets in these integrations were found by performing a backward integration of the planets only, starting from their current configuration. During this 10^7 year integration, we applied a fictitious acceleration that forced the planets to migrate in the opposite direction to that given above. Jupiter, Saturn, Uranus, and Neptune had semi-major axes of 5.40, 8.77, 16.19, and 23.22 AU, respectively, at the end of this integration. The positions and velocities for the giant planets resulting from this integration were used as the initial conditions for the subsequent migration simulations described below. Since the backward integration is the exact time reversal of the main forward integrations, the planets end up in their current configuration.

In order to illustrate the evolution of the giant planets during our simulation, Figures 1A and 1B show the temporal behavior of Jupiter's semi-major axis for the $\tau = 10^7$ year and the $\tau = 3 \times 10^7$ year runs, respectively. Our integrations were stopped at 10^8 years and 2×10^8 years, respectively, since the duration of the LHB appears to have been shorter than these values. In the next section we describe these integrations in more detail.

IV. Initial Conditions and Numerical Methods

The basic idea that links the formation of Uranus and Neptune to the LHB (Wetherill 1975) is that as these planets started to disrupt the region beyond Saturn, they gravitationally scattered some of the planetesimals in this region inwards toward Saturn. Some of these objects encountered Jupiter and made their way into the terrestrial planet region. A fraction of these objects then impacted the Moon. In our assumed simple scenario for planet formation (see §III for a discussion), this disruption was caused by the formation of Uranus and Neptune themselves. Because Uranus and Neptune are assumed to have formed significantly later than the terrestrial planets, the Moon and terrestrial planets would have experienced an increase in impact rates during this time. For the remainder of this discussion, we adopt this scenario for planet formation^[3].

The fact that the formation of Uranus and Neptune must have triggered the migration of Jupiter and Saturn significantly complicates the issue of whether their formation caused the LHB. Not only would Uranus and Neptune planetesimals have found their way into the inner solar system, but the migration of Jupiter and Saturn would have also changed the dynamical structure of the Solar System. As such, some

[3] Other scenarios for the transport of icy bodies from the outer Solar System have recently been proposed, particularly in the context of explaining the deuterium-to-hydrogen ratio of seawater. Delsemme (2000) has proposed that most of Earth's bombardment came from comets in the 'Jupiter zone', rather than from the Uranus-Neptune region. Jupiter-zone comets, Delsemme claims, would have D/H consistent with the water in Earth's oceans. However, this result should be viewed with some caution since the dynamical lifetimes used by Delsemme are implausibly long (see Holman & Wisdom 1993 and Levison & Duncan 1994). Pavlov *et al.* (1999) suggest that solar wind-implanted hydrogen on interplanetary dust particles provided the low D/H component of Earth's water. See §VI for further discussion.

small body reservoirs that were stable up to this time would have suddenly become unstable, releasing their occupants. Some of these objects would have evolved into the inner Solar System and hit the Moon.

We therefore must study several distinct populations of potential impactors that would have been released by Uranus and Neptune. We chose to study: *i*) Uranus-Neptune planetesimals, *ii*) Jupiter Trojans, and *iii*) main belt asteroids. Our numerical experiments consisted of following the orbits of massless test particles from each of these reservoirs from the time of the disruption of the trans-saturnian disk to after the period of giant planet migration. During our integrations, we calculated the impact rates using Öpik’s equations (Öpik 1951) on the terrestrial planets, including the Moon. Levison et al. (2000) have recently shown that these equations are accurate to within $\sim 30\%$.

As described above, although it is generally agreed that the giant planets migrated as they cleared the small bodies that did not get incorporated into them, the magnitude of the migration is still in question. Thus, although we have adopted Malhotra’s scenario for most of our simulations, as an alternative we performed one set of integrations where the giant planets did not migrate and were in their current configuration for the entire length of the simulation. Since the asteroid belt and Trojans would not have been destabilized during this scenario, we restricted this particular study to only the Uranus-Neptune region.

In all our runs, the test particles’ orbits were integrated under the gravitational influence of the Sun and the four giant planets during and immediately following the period of migration. For our main simulations, we used the *RMVS3* integration scheme (Levison & Duncan 1994), which is based on the method of Wisdom & Holman (1991), but can handle close encounters between particles and planets. In order to increase the computational speed of our integrations, the terrestrial planets were not included. This is a reasonable simplification since all the known

Jupiter-family comets, which are dynamically related to the objects from the Uranus-Neptune region and escaped Trojans, are dynamically controlled by Jupiter. This implies that they have not been significantly perturbed by the terrestrial planets. Thus, we expect the same to be true for the objects in our simulations.

The trajectory of each particle was followed for 10^8 years for the $\tau = 10^7$ year and the *no migration* runs, or 2×10^8 years for the $\tau = 3 \times 10^7$ year runs, unless it was ejected from the Solar System, hit the Sun or a giant planet, or reached a heliocentric distance of 10,000 AU. We stopped following a particle at 10,000 AU because galactic tides and passing stars begin to have significant dynamical effects at this distance (Duncan et al. 1987). Presumably, most of these objects will eventually be ejected from the Solar System or will become part of the Oort Cloud.

Generating the initial conditions for the simulations with migration was complicated by the fact that there was a significant delay between the formation of Jupiter and Saturn and the LHB. As a result, these planets had a significant opportunity to sculpt the distribution of both the Trojans and the asteroid belt before giant planet migration started. Our approach for sowing the test particles in these regions for the main simulations was to perform an initial 10^8 year simulation that allowed Jupiter and Saturn to erode away these regions. These initial simulations included Jupiter and Saturn in their pre-migrated orbits. Uranus, Neptune, and the terrestrial planets were not included. In order to crudely model the presence of Mars, we removed any particle whose perihelion distance dropped below 1.5 AU. The rest of this section is dedicated to the results of these initial integrations, with asteroids and Trojans described separately.

Since the fraction of ejected main belt asteroids that hit the Moon is strongly correlated with initial location in the asteroid belt (Gladman et al. 1997; Zappalà et al. 1998; Morbidelli et al. 2000; see also §V), we divided the asteroid belt into two regions: the *inner* asteroid belt from $2 < a < 3$ AU and the *outer* asteroid

belt from $3 < a < 5$ AU. This allowed us to put fewer test particles in the inner region, thus significantly decreasing computational time. For our pre-migration integration of the inner region, we uniformly distributed the semi-major axes of 30 test particles between 2 and 3 AU. Since, as we describe in detail below, the dominant mechanism for the removal of objects from stable asteroid belt orbits is the action of resonances, the exact values for the initial eccentricities and inclinations of the particles will not qualitatively affect our results, as long as the eccentricities and inclinations are small. Thus we set the particles' initial eccentricities to 0.05 and their initial inclinations were distributed uniformly in $\cos i$ for i between 0 and 5° . The arguments of perihelion, longitudes of ascending node, and mean anomalies for the particles were chosen at random from between 0 and 360° .

At the end of the pre-migration integration 28 of these objects remained in the asteroid belt. For our pre-migration integration of the outer region, we uniformly distributed the semi-major axes of 50 test particles between 3 and 5 AU. Recall that Jupiter is at 5.4 AU in these simulations. The other orbital elements were chosen in the same way as above. At the end of the integration only 12 objects survived. We felt that this number was too small for the main integrations with planetary migration. Therefore, we cloned each of these particles 6 times by adding a random number between 0 and 10^{-4} AU to the x , y , and z positions of the particles. This made a total of 72 test particles initially in the outer asteroid belt for simulations with migration.

The dynamical lifetimes of test particles in our initial asteroid belt integrations are shown in Figure 2A as a function of their initial semi-major axes. The integration time for these simulations was 10^8 years, so any object that is shown to have a dynamical lifetime of 10^8 years (marked by the dotted line in the figure) was actually stable. In these cases, 10^8 years is a lower limit to the dynamical lifetime. For comparison, Figure 2B shows the results of a similar set of integrations, except

that the giant planets were in their current configuration. The locations of the ν_6 secular resonance and the 2:1 and 3:1 mean motion resonances with Jupiter are shown in the figures. As has been known for many years (e.g. Wisdom 1983; Murray 1986), objects in these resonances are not stable.

A comparison between the two panels in Figure 2 shows that the locations of the resonances are different in the two planetary configurations. In particular, in the pre-migrated system, the resonances are further from the Sun than in the current Solar System. This is easy to understand for the mean motion resonances with Jupiter. Jupiter is further from the Sun, so its orbital period is longer. Since the mean motion resonances are places where the orbital period of a small body is commensurate with that of Jupiter, they must also be further away from the Sun.

The ν_6 resonance is also further from the Sun in the premigrated case. Indeed, it is shifted much more than the mean motion resonances. This is due to a combination of two effects. First, the precession rate of objects in the asteroid belt is primarily determined by their distance from Jupiter. The ν_6 secular resonance is located where the precession frequency of an asteroid is the same as the g_6 eigenfrequency of the Laplace-Lagrange solution for the secular variations of the planets (approximately the precession frequency of Saturn). Since Jupiter is further from the Sun, this location must also be further from the Sun. Second, since Jupiter and Saturn are closer to one another, the g_6 frequency is larger. Objects in the ν_6 must therefore have larger frequencies and thus must be even closer to Jupiter. As result, the ν_6 resonance is near 3.1 AU in the pre-migrated Solar System for small inclinations, while it is near 2.1 AU in the current Solar System.

It should be noted, however, that the location of the ν_6 secular resonance is very sensitive to the exact locations of the giant planets (particularly Jupiter and Saturn). This sensitivity is due to the fact that in our pre-migrated system, Jupiter and Saturn are near the 2:1 mean motion resonance (the ratio of their orbital periods

is 2.07). As a result, the precession frequency that causes the ν_6 resonance is much more strongly affected by the location of the planets than it would be if the resonance were not present. According to the numerical integrations of Gomes (1997), if our initial conditions had put Saturn 0.1 AU further from the Sun, the location of the ν_6 resonance would be roughly 0.5 AU closer to the Sun. If, on the other hand, our initial conditions had Saturn 0.1 AU closer to the Sun, the location of the ν_6 resonance would move outward by almost 1 AU! So, with very modest differences in our initial conditions, the location of the ν_6 would be very different. This issue is exacerbated by the fact that since our small objects are being treated as massless test particles, the mass of the trans-saturnian proto-planetary disk is not included in these calculations. This too would affect the location of the ν_6 . These facts should be considered when interpreting the results of our integrations.

Given the above results, we can now predict what we will see when we analyze the simulations of the asteroid belt as Jupiter and Saturn migrate. The locations of the resonances will migrate from their locations shown in Figure 2A to those in Figure 2B. In addition to the resonances that are marked in the figure, higher order mean motion resonances are spread throughout the region, particularly outside the 2:1. These will also migrate inward. As the resonances sweep through regions that were initially stable, asteroids will be kicked out of the asteroid belt. Indeed, this same mechanism has been proposed to explain the paucity of asteroids observed beyond the 2:1 (Liou & Malhotra 1997) and the large eccentricities and inclinations of main belt asteroids (Gomes 1997). Some of the escaped asteroids will impact the Moon and terrestrial planets.

We may be leaving important effects out of the above discussion, and indeed, out of our simulations. For example, if at this point in the history of the Solar System, the asteroid belt had a significant amount of mass, then that mass would have also changed the precession frequencies of the asteroids. The precession

frequencies of small bodies embedded in a massive disk are decreased due to the disk’s gravity (Ward 1980, Lecar & Franklin 1997). As a result, if the asteroid belt were massive at the time corresponding to the beginning of our simulations, the ν_6 secular resonance would be even further from the Sun than the 3.1 AU discussed above. So, even more damage to the asteroid belt would have been done as the ν_6 evolved to its current location. On the other hand, if the asteroid belt were massive enough and the eccentricities were small enough, then density waves would have been excited at resonances (Goldreich & Tremaine 1982; Ward & Hahn 1998a,b). These waves might have stabilized objects in the mean motion resonances and the ν_6 secular resonance, in which case the Moon would not have been struck by as many asteroids as the giant planets migrated. In addition, collisions would have been more frequent in a more massive belt; such collisions could also have damped eccentricities. We ignore these effects in the simulations discussed here, but revisit these issues in the next section.

For our pre-migration integration of the Trojans, we uniformly distributed the semi-major axes of 350 test particles between 5.2 and 5.6 AU. (Again, Jupiter is at 5.4 AU in these integrations.) The other orbital elements were chosen in the same way as described above. Not all the particles generated using these procedures will be in the Trojan 1:1 mean motion resonance because we are uniformly picking the angles. However, these particles will uniformly cover the entire region of the resonance, which is our desired result. We find by examining the results of this integration that 204 out of the original 350 were librating in the 1:1 mean motion resonance at the beginning at the integration.

None of the librating particles survived the 10^8 year pre-migration simulation. Particles that were initially in the 1:1 resonance with Jupiter follow a behavior similar to the unstable Trojans in the current Solar System (Levison et al. 1997) — at the end of their dynamical lifetimes, their libration amplitude increases

monotonically until the particles start to encounter Jupiter. During this time, the particles' proper eccentricities remain approximately constant. Figure 2 of Levison et al. (1997) shows an example of this type of evolution.

The instability of the Trojans is clearly a problem with our standard model for Solar System formation since it would predict that no Trojans should exist. One possibility is that the Trojan swarms were several orders of magnitude more massive than we see today ($< 1/204$) survive the pre-migration stage of formation; $\sim 3\%$ survive the migration, see below; and even fewer survive to modern times because of dynamical erosion (Levison et al. 1997) and physical collisions (Marzari et al. 1996). This seems improbable.

On the other hand, the result that the Trojan swarms are unstable is very sensitive to our choice for the locations of Jupiter and Saturn. Gomes (1997, 1998) points out that if Jupiter and Saturn originally orbited at 5.4 and 8.7 AU, respectively, they would have been almost in a 2:1 resonance with each other. Such a near-resonance may have destabilized the Trojans in the simulation we just described. We ran an experiment similar to the one above, except that Jupiter and Saturn had semi-major axes of 5.3 AU and 9.0 AU, respectively. Approximately 20% of the objects survived for 10^8 years. Thus, a slightly different set of initial conditions could have resulted in the stability of the Trojan swarms. Although the existence of the Trojan swarms could be used as a constraint for the structure of the pre-migrated Solar System (Gomes 1998), a detailed investigation is beyond the scope of this paper and will be left for future work.

Even though the Trojan swarms would not have survived in our standard model of Solar System formation, we decided not to modify the model in our main simulations below. We reached this decision because it was not clear how to modify the standard model in a way consistent with constraints on the physics of planet migration (such as the conservation of energy and angular momentum) and the

observed constraints. In addition, we believe that the results of the simulations with migration will not, at least qualitatively, be affected by our choice of pre-migration planetary orbits. (Indeed, below we show this to be true for the Uranus-Neptune zone.) Thus, we generated the initial conditions of our swarm from the 10 particles that survived in our pre-migration integration for 5×10^7 years. Six of these particles were in the L_4 swarm and four were in the L_5 swarm. Therefore, we cloned each of these particles 30 times, making a total of 300 test particles initially in the Trojan regions for simulations with migration.

V. Results of the Integrations

As described above, we performed a series of integrations that covered a variety of small-body reservoirs and different migration times, τ . We studied three reservoirs: *i*) the asteroid belt, *ii*) Jovian Trojans, and *iii*) Uranus/Neptune planetesimals. We chose to study $\tau = 10^7$ years and 3×10^7 years. In addition, we studied a system with no migration for the Uranus-Neptune reservoir. Table 1 shows the fraction of objects from each of these reservoirs that struck the Moon in the first 10^8 years of the main integrations. These values were calculated using Öpik’s equations (Öpik 1951).

Table 1
Fraction of Objects Impacting the Moon in the First 10^8 Years

Reservoir:	Asteroid Belt	Trojans	Uranus-Neptune
$\tau = 10^7$ year	2×10^{-4}	5×10^{-8}	1×10^{-8}
$\tau = 3 \times 10^7$ year	4×10^{-4}	9×10^{-8}	8×10^{-9}
No migration	—	—	2×10^{-8}
Mass Required [†]	2×10^{25} g	9×10^{28} g	7×10^{29} g

† The mass required in the region in order for the Moon to have accreted 6×10^{21} g of material from that region alone. These values are averages of the two migration runs only.

The differences between the $\tau = 10^7$ year, $\tau = 3 \times 10^7$ year, and no migration runs for the same reservoir are most likely due to small number statistics. Table 1 also lists the amount of mass required in each at the beginning of the migration in order for the Moon to have accreted 6×10^{21} g. These numbers were obtained by averaging the results of the $\tau = 10^7$ and $\tau = 3 \times 10^7$ year runs. We now discuss the details of the dynamics of objects leaving each reservoir separately, starting with the most distant and working inward.

Uranus-Neptune Planetesimals

We integrated the orbits of 200 massless test particles initially in the Uranus-Neptune zone under the gravitational influence of the giant planets. The particles were initially distributed uniformly in semi-major axis between 15 and 32 AU except that particles were not placed in the classical instability strips of the planets as defined by Wisdom (1980). The other orbital elements for these objects were chosen using the procedures described above.

One aspect that is critical in evaluating whether these objects could have been the cause of the LHB is the temporal distribution of impacts on the Moon. Figure 3 shows histograms of the impact rate (fraction of objects hitting the Moon over a 2 million year period) as a function of time in our runs. The trends seen in the three distributions are similar. The vast majority of impacts on the Moon from these objects occur in the first 1.5×10^7 years. It is important to note that the number of particles in our simulations that ever evolve onto orbits with perihelion distances < 1 AU is small, $\sim 5\%$, so that much of the high frequency structure seen in the figure is probably due to small number statistics [4].

In the run with no migration (Figure 3c) there is a low level of impacts at times later than 3×10^7 years. This is due to particles that were initially scattered to large semi-major axes and are slowly leaking back into the planetary region. Such objects exist in all three of the runs. After 10^8 years, 20% of the particles in each of the ‘no migration’ and $\tau = 10^7$ year runs are found at large semi-major axes, while the value is 12% in the $\tau = 3 \times 10^7$ year run. Thus we believe if we had integrated enough particles, all three runs would have shown a low level of impacts at late

[4] If the Uranus-Neptune region contained some large objects besides Uranus and Neptune, the migration itself could have been non-uniform and thus the impact flux might also have been non-uniform.

times.

The data in Figure 3 imply that the destabilization of the Uranus-Neptune region could indeed have caused a very narrow spike in the impact rate on the Moon and thus could have caused the LHB. The fact that the timescale for the influx is approximately independent of whether or not there was migration (and, if there was, its rate) supports this hypothesis. This result is not surprising because it is well known that the region between Uranus and Neptune in the current Solar System is unstable on a timescale of $\sim 10^7$ years (Gladman & Duncan 1990; Holman & Wisdom 1993). Thus, the influx that we are seeing is only a result of this clearing and is largely independent of the migration^[5].

Another diagnostic for determining whether the LHB could have arisen in this region is provided by estimating the number of objects and the total amount of mass initially required in the Uranus-Neptune region to account for the amount of material impacting the Moon. As described in §II, at least twelve ~ 30 km bodies and at least two ~ 110 km bodies hit the Moon during the LHB, and the impactors that created the late basins had a total mass of approximately 6×10^{21} g. If all of this material came from the Uranus-Neptune region, the efficiencies given in Table 1 imply that the Uranus-Neptune region must have contained $(1.2\text{--}1.5) \times 10^9$ 30-km bodies, $(2.0\text{--}2.5) \times 10^8$ 110-km bodies, and a total initial mass (not including the planets) of $\sim 7 \times 10^{29}$ g. The combined mass of Uranus and Neptune is 2×10^{29} g. Thus, if the assumptions outlined above are correct, of the material initially in the Uranus-Neptune region, $\sim 20\%$ was accreted by the planets. The rest was either ejected from the system or placed in the Oort Cloud. This relatively

[5] This argument is not robust, however. If the migration were very quick, we would probably see a correlation between the width of the spike and the migration time. In addition, as we described in §III, if Uranus and Neptune grew very slowly, the timescales could be lengthened.

low accretion efficiency is in general agreement with orbital simulations of objects in the Uranus-Neptune region, which suggest that most bodies in this region should be ejected from the Solar System or placed in the Oort Cloud or scattered disk (Safronov 1972; Shoemaker and Wolfe 1984; Duncan et al. 1987; Lissauer et al. 1995; Hahn & Malhotra 1999; Levison et al. 1999; Dones et al. 2000).

If 6×10^{21} g of water-rich bodies from the Uranus-Neptune region hit the Moon at 3.9–3.8 Ga, the Moon might retain a small fraction of this water today. Polar ice on Mercury has been inferred by ground-based radar experiments (Slade et al. 1992, Harmon et al. 1994). Arnold (1979) argued that the poles of the Moon should harbor $\sim 10^{16}$ to 10^{17} g of water. The Clementine radar experiment tentatively detected small amounts of water ice near the Moon’s south pole (Nozette et al. 1996), although this result has not been confirmed by other groups (Stacy et al. 1997; Simpson and Tyler 1999). Recently Feldman et al. (1998) have inferred from Lunar Prospector Neutron Spectrometer data that as much as 3×10^{15} g of ice may lie beneath the lunar surface near each pole. Our results suggest that 10^6 times as much ice may have impacted the Moon during the Late Heavy Bombardment.

The issue is how much of the water the Moon retained after an impact, i.e. whether it can retain a transient hydrostatic atmosphere of hot steam. A hydrostatic adiabatic (polytropic) atmosphere will have a finite density at infinity if $H_0/R_p > (\Gamma - 1)/\Gamma$, where $H_0 \equiv kT_0/mg$ refers to the scale height at the ground, R_p refers to the radius of the planet, Γ is the ratio of specific heats (not to be confused with γ , the index of the impactors’ mass distribution), k is Boltzmann’s constant, m is the mass of a molecule in the atmosphere, and g is the Moon’s surface gravity. A finite density at infinity means that the atmosphere cannot be static; rather, it blows off to space on a dynamical time scale. Water generated from the impactor will initially be quite hot. Consider ice. In a planar impact of similar substances, the internal energy deposited in the impactor is roughly $v_{\perp}^2/8$, where

v_{\perp} refers to the normal component of the impact velocity v (Melosh 1989, p. 57). Assuming $v = 16$ km/s and $v_{\perp} = v/\sqrt{2} \sim 11$ km/s, a latent heat of vaporization of 3×10^{10} erg/g, $\Gamma = 1.33$, and a specific heat of $(\Gamma/(\Gamma-1))(k/m) \sim 1.8 \times 10^7$ erg/g/K (where m is the mass of a water molecule), we estimate that the steam would be about ~ 7000 K. For the Moon this gives $H_0/R_p \approx 1.2$, which is much larger than $(\Gamma - 1)/\Gamma = 0.25$. Thus we conclude that most of the water vapor is lost. Dissociation of water only lowers the molecular weight, making retention even less likely.

In addition, the Moon would only retain water in permanently shaded polar regions. The Moon may not have had its current obliquity at the time of the LHB (Ward 1975, Moses et al. 1999, Vasavada et al. 1999); thus there may not have been permanently shaded regions at that time.

We can also use our simulations to estimate the cratering rate on various solid bodies in the inner Solar System. If the cratering records on these objects were well enough understood (which is not currently the case, see §I), the relative cratering rates could be used as an important diagnostic for the LHB. Table 2 lists and Figure 4A shows R , the ratio of the impact rate (number/km²) on a planet relative to that on the Moon. These numbers were arrived at by dividing the total number of impacts that our simulations predict should have occurred on a planet, including gravitational focusing, by the planet's surface area. So, R is the relative number of impacts per unit area on different planets. The scaling of the relative amount of *mass* impacting different planets depends upon the impactors' mass distribution. If we assume a cumulative distribution $N(> m) \propto m^{-\gamma}$, most of the mass is in the smallest bodies if $\gamma > 1$, and in the largest bodies if $\gamma < 1$. If $\gamma > 1$, the expected mass is just proportional to the number of impacts. That is, the expected mass impacting the planet is RA times that accreted by the Moon, where A is the ratio of the planet's physical area to the Moon's. If $\gamma < 1$, a more massive planet

is likely to suffer a more massive impact, and the expected impacting mass is of order $(RA)^{1/\gamma}$ times the mass striking the Moon. See Anbar et al. (2000) for further discussion. We present our data in this way because the size distribution of the impactors is unknown.

Table 2
Number of Impacts per Unit Area, Relative to the Moon

Planet	Uranus-Neptune			Trojans		Asteroid Belt	
	10^7	3×10^7	NM [†]	10^7	3×10^7	10^7	3×10^7
Mercury	0.19	0	0.46	0.31	0.88	0.81	0.80
Venus	0.45	0.12	0.89	1.11	1.41	1.40	1.68
Earth	1.72	1.50	1.37	1.44	1.43	1.64	1.61
Mars	2.19	3.34	1.29	2.81	0.90	1.83	0.99

† No migration run.

The parameter R does not include any differences in crater densities that would arise due to differences in impact velocities or atmospheric filtering. Although our simulations supply no insight into the impactor size distribution, they do supply us with impact velocities. Table 3 lists our prediction for the average velocity (v_∞) that an impactor will have at large distances from the planet. Since we do not believe that the cratering record on the other terrestrial planets is well enough understood for us to interpret these values, we present these data in the hope that they may be useful to future investigators.

Table 3
Mean Encounter Velocity of Impactors (km/sec)

Planet	Uranus-Neptune			Trojans		Asteroid Belt	
τ (years)	10^7	3×10^7	NM [†]	10^7	3×10^7	10^7	3×10^7
Mercury	33.3	—	38.0	33.8	35.7	33.0	29.8
Venus	21.5	23.3	24.5	20.5	25.1	22.1	20.9
Earth	14.7	16.2	20.7	18.6	20.6	17.3	17.7
Mars	15.4	12.7	16.0	13.8	17.7	11.5	13.8

† No migration run.

The steep increase in predicted impact rate per unit area with heliocentric distance for small bodies from the Uranus-Neptune region is due to the distribution of encounter velocities that objects have with Jupiter ($v_{J,enc}$). To first approximation, the magnitude of the encounter velocity is conserved during an encounter (this value is related to the Tisserand parameter). Jupiter can change a small body’s direction, but not its relative speed. If the encounter velocity is very small, then the orbit of an object is very close to that of Jupiter, and Jupiter cannot change the orbit enough for it to cross the orbit of one of the terrestrial planets.

Figure 5A shows the fraction of encounters with Jupiter that lead to orbits that cross the orbits of terrestrial planets as a function of the ratio of the encounter speed to Jupiter’s mean orbital velocity, U . For small values of U the fractions are zero, while for larger U , they increase as U increases. The solid curve in Figure 5B is the cumulative distribution of U for the $\tau = 10^7$ year integration. A comparison of the two plots shows why there is a strong relationship between the heliocentric distance of a planet and its impact rate for the Uranus-Neptune planetesimals. More objects can reach Mars than can reach Earth and more objects can reach Earth than Venus.

The existence of an ancient, massive (e.g., one-to-several bar CO₂) atmosphere on Mars could be another constraint on the LHB. Such an atmosphere appears to

be required to create the pressure-temperature conditions necessary to support the ancient surface water revealed by martian geology (cf. Pollack et al. 1987). Baker et al. (1991) proposed that many of the water-derived surface morphologies can be explained by brief martian greenhouse periods. More recently, Gulick et al. (1997) have studied this hypothesis in some detail, showing that pulses of CO₂ injection of 1 to 2 bars can indeed place the martian environment into a quasi-stable, greenhouse state, with surface temperatures in the range 240 to 250 K for several hundreds of Myr. The process responsible for generating such CO₂ injection pulse(s) has been difficult to identify, and there are problems with all of the ‘internal’ (i.e., martian) mechanisms.

Stern & Levison (1999) described how a 1 bar CO₂ atmosphere can be produced by the accretion of $\sim 3 \times 10^{22}$ g of cometary material. Our simulations show that Mars accretes between 5 and 13 times as much mass as the Moon depending on the run if $\gamma \geq 1$, and 7–21 times as much if $\gamma = 5/6$. Assuming the average of 10 and that the Moon accreted 6×10^{21} g of cometary material during the LHB, we estimate that Mars should have accumulated $\sim 6 \times 10^{22}$ g of material, consistent with the estimates of Stern & Levison (1999).

Finally, the origin of Earth’s water is of great interest (Lecuyer et al. 1998, Righter et al. 1999, Abe et al. 2000). It has been suggested that the volatiles of Earth could also have been a result of the LHB (Chyba 1990; Chyba et al. 1994). The scenario that the LHB was caused by Uranus-Neptune planetesimals, which we assume were comet-like and contained $\sim 50\%$ water ice, again raises the issue as to whether the oceans of Earth could have been delivered by comets. The oceans of Earth contain $\sim 1.4 \times 10^{24}$ g of water (Walker 1977) and the interior of the Earth may contain even more (Dreibus & Wänke 1989). Our simulations show that $\sim 2 \times 10^{-7}$ of the objects originating between Uranus and Neptune hit the Earth during the LHB. Given our nominal value of $\sim 7 \times 10^{29}$ g of material in the Uranus-Neptune

zone, as described above, the Earth would have accreted $\sim 7 \times 10^{22}$ g of water (assuming the impactors were 50% water ice by mass), which is roughly 5% of its oceans. Indeed, in order for these objects to have been the sole source of Earth’s oceans, there must have been at least 10^{31} g ($\sim 2000M_{\oplus}$) of material in the Uranus-Neptune zone, assuming that $\gamma \geq 5/6$. This is an unreasonable amount of material, as first pointed out by Zahnle (1998). Thus, it is unlikely that Earth’s oceans could have been accreted by this mechanism, unless the planetesimals’ size distribution was extremely shallow ^[6]. However, such a shallow distribution is very unlikely.

Our results are consistent with recent measurements of the deuterium to hydrogen ratio in three comets believed to have come from the Oort Cloud. In these comets – Halley, Hyakutake, and Hale-Bopp – D/H is ~ 3 times higher than the measurement for Earth (Meier & Owen 1999). Many or most Oort Cloud comets are believed to have originated in the Uranus-Neptune zone (Duncan et al. 1987). If these D/H values are representative of the Oort Cloud, it is unlikely that a significant amount of Earth’s water came from Uranus-Neptune planetesimals. Most of Earth’s water may have come from Jupiter-zone planetesimals (Zahnle 1998, Delsemme 2000) or the outer asteroid belt (Morbidelli et al. 2000) prior to the LHB, or from solar-wind implanted interplanetary dust particles (Pavlov *et al.* 1999).

Jupiter Trojans

We integrated the orbits of 300 massless test particles initially in the 1:1 mean motion resonance with Jupiter under the gravitational influence of the giant planets

[6] For instance, if $\gamma = 1/2$, only $100M_{\oplus}$ in the Uranus-Neptune zone would be required. In this case roughly half the water would likely have been carried by the largest impactor (Tremaine & Dones 1993).

as they migrated. We followed the orbital evolution of these objects until either they were ejected from the Solar System, entered the Oort cloud, or impacted the Sun or a giant planet.

The temporal evolution of the impact rate on the Moon due to escaped Trojans is given in Figures 6A and 6B for the $\tau = 10^7$ year and $\tau = 3 \times 10^7$ year runs, respectively. As is the case for Uranus-Neptune planetesimals, in these simulations the Moon experiences a narrow peak in the impact rate with a duration of 10 to 20 million years. From Table 1, we find that the fraction of objects from the Trojan swarms that impacts the Moon is $\sim 7 \times 10^{-8}$. If we assume that all of the LHB came from this region of the Solar System, then at the beginning of the migration it must have contained $\sim 6 \times 10^{21} \text{ g} / 7 \times 10^{-8} = 9 \times 10^{28} \text{ g}$, which corresponds to $14M_{\oplus}$. This is a lower limit to the amount of material that must have initially been in the swarm at the time of Jupiter's formation in order to produce the LHB, since a swarm this massive would have evolved substantially due to dynamical erosion (see above) and collisional evolution (Marzari et al. 1996) in the ~ 700 million years between the time when the swarm formed and the migration started. Thus, we must conclude that in order for the Trojan swarms to be an important source for the LHB, they must have contained more mass than the solid core of Jupiter (Guillot 1999), which we believe is unlikely. Thus, it seems that escaped Trojans must have played at most a minor role in the LHB.

Figure 4B and Table 2 show the impact rate per unit area on the terrestrial planets relative to the Moon, as predicted by our simulations. Note that the variation with respect to heliocentric distance is much shallower than that observed for Uranus-Neptune planetesimals (Figure 4A), particularly between Venus and Earth. Recall that for Uranus-Neptune planetesimals, the steep spatial distribution is due to the narrow distribution in the encounter velocity with respect to Jupiter. We were initially somewhat surprised that the distribution for the escaped Trojans

was shallower, since when Trojans escape the swarms, they have much smaller Jupiter encounter velocities. However, the observed distribution of U for escaped Trojans, which is shown by the dashed curve in Figure 5B, shows a distinct tail for $U \gtrsim 0.8$, which causes the shallow gradient in impact rate per unit area.

A detailed study of the behavior of escaped Trojans on terrestrial planet-crossing orbits shows that they must first encounter Saturn (and perhaps Uranus and Neptune) before entering the terrestrial planet region. When objects first leave the Trojan swarm, their encounter velocities are so small that Jupiter is unlikely to kick them into terrestrial planet-crossing orbits (cf. Figure 5A), nor can it eject the particles from the Solar System. The only way Jupiter can remove these particles is for it to hand them to Saturn. Saturn can then kick the particles out of the Solar System, or hand them off to Uranus or Neptune. Saturn can also hand them back to Jupiter, at which point their U would have been increased so that Jupiter can hand them down to the terrestrial planets. Thus, any escaped Trojan in our simulation that became terrestrial planet-crossing must have first encountered Saturn.

Although it is unlikely that Trojans played an important role in the LHB, they are an important diagnostic of early Solar System formation. In particular, their existence places an important constraint on the pre-migrated structure of the Solar System and the era of planetary migration. For example, as described above, Trojans are not stable in our standard pre-migrated Solar System for $\gtrsim 10^8$ years, though they are stable for slightly different initial orbits for Jupiter and Saturn (§IV). Also, the fraction of objects that survive the migration is dependent on τ , and thus τ can be constrained by the existence of the Trojans (see Gomes (1998) for a more complete discussion).

The Asteroid Belt

As discussed in §IV we subdivided the asteroid belt into two regions for our

simulations. The inner region ($2 < a < 3$ AU) initially contained 28 particles. The outer region ($a > 3$ AU) initially contained 72 particles (12 particles cloned 6 times). As with the previous sets of runs, we followed each particle until it was either ejected from the system, hit the Sun or a planet, reached 10^4 AU, or the end of the simulation was reached: 10^8 years for the $\tau = 10^7$ year integration and 2×10^8 years for the $\tau = 3 \times 10^7$ year run. We combine the results from the two regions of the asteroid belt in the analysis below.

The temporal evolution of the impact rate on the Moon due to escaped asteroids is given in Figures 7A and 7B for the $\tau = 10^7$ year and $\tau = 3 \times 10^7$ year runs, respectively. Importantly, unlike the previous cases studied, the timescale for the peak in the lunar impact rate is directly correlated with the migration rate for the planets. This is because the migration of the ν_6 secular resonance is mostly responsible for exciting objects out of the asteroid belt and into Earth-crossing orbits, and the location of the ν_6 is directly related to the location of the giant planets.

The above point is illustrated in Figure 8, which shows the dynamical lifetimes^[7] as a function of their initial semi-major axes in the asteroid belt in our $\tau = 10^7$ year run. The migration of the ν_6 secular resonance and the Jovian 2:1 and 3:1 mean motion resonances are shown. Note that the region between 2.1 and 3.2 AU is mostly cleared by the motion of the ν_6 resonance. Indeed, the migration of this secular resonance can be seen in the dynamical lifetimes of the objects: those closer to the Sun have longer lifetimes. The exception to this is near the location of the 3:1 mean motion resonance with Jupiter. Here, the resonance itself

[7] By dynamical lifetime we mean the length of time between the start of the simulation and the time that a particle is removed from the Solar System. It does not refer to the time it takes for a particle to be removed from the asteroid belt.

determines the precession rates of the objects in it, so the ν_6 does not penetrate and the particles are stable. The small dip in the impact rate seen in Figure 7B at $\sim 6 \times 10^7$ years, and perhaps even the one in Figure 7A at $\sim 1.5 \times 10^7$ years, are due to the passage of the ν_6 over the 3:1.

Referring back to Figure 7, the constant impact rate at $t > 10^8$ years seen in the $\tau = 3 \times 10^7$ year run is due to a single particle that has its eccentricity increased by the ν_6 resonance until it crosses the orbits of Mars and Earth, but was far enough from the center of the resonance that it was not driven into the Sun. (Becoming a Sun-grazer is the most common fate of objects in the ν_6 .) This particle is very long-lived because its aphelion distance is far inside the orbit of Jupiter, and there are no terrestrial planets in our integrations. In the real Solar System, the terrestrial planets would remove such a particle (Gladman et al. 2000). Therefore, we ignore this particle for the remainder of this discussion.

It is well known that the amount of mass currently in the asteroid belt ($\approx 4 \times 10^{-4} M_\oplus$) is small compared to the amount predicted to be there by extrapolating the disk necessary to form the terrestrial planets ($\sim 6 M_\oplus$, Weidenschilling 1977). One of the mysteries of planetary science is what happened to this material. Several mechanisms have been discussed, including the sweeping of the ν_6 secular resonance (Ward 1980; Lecar & Franklin 1997). In this model, a massive asteroid belt is invoked to decrease the precession frequencies of the asteroids, thereby moving the ν_6 outward. As the mass in the asteroid belt decreases, the ν_6 sweeps inward. Here we present a different, but complementary, argument, similar to that of Gomes (1997), for why the ν_6 may have migrated through the asteroid belt and effectively cleared it out.

Both our model and Ward's model suffer from the same limitations. If the asteroid belt were massive enough, then two mechanisms could prevent the growth of the eccentricities of objects in the ν_6 resonance. In a massive disk, collisions

between asteroids will be frequent. As the ν_6 migrates past a location and particles start to get excited, collisions with nearby non-resonant particles could remove the particles from the resonance. This could damp the growth of eccentricities. In addition, if the eccentricities of the asteroids were small, then the ν_6 would generate waves in the asteroid belt (Ward & Hahn 1998b) that allow angular momentum to be shared among a good fraction of the asteroids in the belt. So rather than the torque of the secular resonance affecting the angular momentum of only the objects in it, the wave would spread that torque all over the disk. These waves could effectively stabilize objects in the ν_6 secular resonance.

Indeed, one of these mechanisms must have been active if our standard model of planet formation is to be correct. One of the disturbing aspects of Figure 8 is that the ν_6 secular resonance is so effective at removing particles as it sweeps by. Our simulations would appear to predict that there should not be any asteroids between ~ 2.1 and $\sim 3.1 AU$ except near the 3:1 mean motion resonance^[8]. Perhaps one way around this problem is to change the initial locations of the giant planets. As described in §III, the initial location of the ν_6 is very sensitive to the exact location of Jupiter and Saturn. By small changes in our initial conditions, we may be able to bring the initial location of this resonance in to $\sim 2.5 AU$ (see Gomes 1997, Figure 3). While this helps to alleviate this problem somewhat, we still need to invoke some mechanism that will make the removal of objects by the ν_6 less efficient.

At the time of the LHB, the mass of the asteroid belt was, of course, somewhere between its current value of $\sim 4 \times 10^{-4} M_\oplus$ and its assumed primordial value of $\sim 6 M_\oplus$. Combining these values with the impact efficiencies presented in Table 1

[8] It should be noted that Gomes (1997) found that the ν_6 would leave some particles behind if the migration times were very short, $\lesssim \text{few} \times 10^6$ years. However, these migration times seem to be inconsistent with recent numerical integrations of this process (Hahn & Malhotra 1999).

suggests that the amount of material that the Moon would have accreted under our adopted scenario is between $8 \times 10^{-8} M_{\oplus}$ (5×10^{20} g) and $2 \times 10^{-3} M_{\oplus}$ (10^{25} g). The latter number clearly violates the observational constraints on the LHB discussed in §II. Indeed, this seems to argue that the ν_6 could not have been directly responsible for the removal of primordial mass in the asteroid belt if that removal occurred after the Moon solidified. It does not, however, prove that the asteroid belt was not massive at the time of the LHB, since as we describe above, there are mechanisms that might inhibit the effectiveness of the ν_6 .

At the other extreme, if the asteroid belt had already reached its current mass by the time of the LHB, then the amount of asteroidal material accreted by the Moon would have been an order of magnitude smaller than our estimate of the amount of material that hit the Moon during the LHB (6×10^{21} g). In this case, the LHB could have been a combination of comets from the Uranus-Neptune zone and asteroids from the main belt. For this scenario to be correct requires the mass in the asteroid belt at the time of the LHB to be less than ten times its current mass.

If, on the other hand, we assume that the asteroid belt was entirely responsible for the LHB, we can estimate its mass at the time: 2×10^{25} g. This is approximately an order of magnitude larger than currently observed, but roughly three orders of magnitude smaller than the assumed primordial value.

VI. Concluding Remarks

As part of an ongoing program to study various scenarios for the lunar ‘Late Heavy Bombardment’ (LHB), we investigate the hypothesis that it resulted from the formation of Uranus and Neptune. The model for the formation of the planetary system that we adopt assumes that the terrestrial planets, Jupiter, and Saturn formed at approximately the same time, 4.6 – 4.5 billion years ago. Uranus and Neptune’s formation was assumed to be delayed until about 3.9 billion years ago, after which time they formed quickly (see §III for a more detailed discussion). In this scenario, Jupiter and Saturn formed with semi-major axes of 5.4 AU and 8.8 AU, respectively. When Uranus (at 16.2 AU) and Neptune (at 23.2 AU) then formed, they started scattering neighboring icy planetesimals throughout the solar system – forming the Oort cloud and causing the LHB on the terrestrial planets. In addition, this scattering process caused the giant planets to migrate to their current locations. Finally, the migration of the giant planets destabilized objects in the Trojan swarms of Jupiter and in the asteroid belt. These objects could also have contributed to the LHB.

We make two assumptions in evaluating the implications of our numerical experiments. They are: (1) The LHB represents a spike in the impact history of the Moon lasting $\lesssim 100$ million years. (2) Approximately 6×10^{21} g of material hit the Moon during the LHB.

The numerical experiment that we performed on the behavior of Uranus-Neptune planetesimals following a late formation of these planets shows that lunar impacts from these objects meet our constraints for the LHB. Uranus-Neptune planetesimals would have arrived at the Moon in a tight spike that could have lasted as short as 10 million years after the time of the formation of Uranus and Neptune. If we assume that the formation of Uranus and Neptune was 20% efficient, then the Uranus-Neptune region must have initially contained 5 times the current mass of

these planets of $31M_{\oplus}$ (1.9×10^{29} g). Our integrations show that the Moon would have accreted about 6×10^{21} g, in agreement with our constraints. This result is roughly independent of the rate of migration. Indeed, a run with no migration and with the giant planets at their current locations produces results similar to our primary integrations.

In this model, Mars would have accumulated $\sim 6 \times 10^{22}$ g of material. This amount of icy material could have produced a temporary CO_2 atmosphere with surface pressures greater than 1 bar (Stern & Levison 1999), which could, in turn, explain Mars' putative early wet environment (Gulick et al. 1997).

It is unlikely that Earth could have accumulated enough water during this event to account for its oceans. However, small number statistics — which are inescapable for any mass distribution in which most of the mass is in the largest bodies (Tremaine & Dones 1993, Zahnle & Sleep 1997, Anbar et al. 2000) — allow that the Earth could have been hit by a large object that did deliver an ocean's worth of water. However, our conclusion is consistent with recent measurements of the deuterium to hydrogen ratio in comets, which is ~ 3 times higher than the measurement for Earth (Meier & Owen 1999). If these new measurements are representative, then it is unlikely that a significant ($\gtrsim 10\%$) amount of Earth's water came from comets.

The late bombardment of the terrestrial planets would have been accompanied by an even heavier impact flux onto the moons of the giant planets. Such a bombardment would have had a profound effect on the galilean satellites, presumably long after they had formed, and might well have shaped attributes of their surface layers in ways still manifest today, especially for the more ancient crusts of Ganymede and Callisto.

From our integrations we estimate that the rate at which craters of a given size formed on the galilean satellites during the LHB was 40 times higher on Callisto,

and 110 times higher on Ganymede, than the rate at that time on the Moon (also see Table I of Zahnle et al. 1998). We focus on Callisto because it has the oldest surface. The dozen 300-km and larger late lunar basins translate to some 500 basins on Callisto. The larger of these impacts would have geometrically saturated Callisto's surface with basins. The bombardment also could have melted the satellite's surface to a considerable depth. Of the 500 basins that we estimate would have formed, perhaps 50 would be roughly Imbrium-scale. For an Imbrium-scale impact on Callisto, we estimate that 5% of the impact energy, or 10^{32} ergs, goes into melting the moon's surface. If we assume that Callisto's surface is made of ice, the resulting mass of water is 3×10^{22} g. If we approximate the melted region as a hemisphere, the maximum depth is 125 km. Thus it seems possible that impacts during the LHB would have melted much or all of Callisto's surface to a depth of 100–150 km. In this view, most of the basins that formed during the LHB would be (at best) difficult to recognize at present. Thus the observation that only four or so large basins are known on Callisto (Schenk & Moore 1999) may be consistent with our model. Crater counts suggest that Lofn on Callisto and Gilgamesh on Ganymede postdate the LHB (Zahnle et al. 1998, Wagner et al. 1999, Zahnle et al. 2001). We will carry out detailed comparisons with the impact history of the outer Solar System in future work.

The Trojan swarms would not have contributed much material to the LHB as Jupiter migrated inward. The efficiency with which objects evolve onto Earth-crossing orbits is very low because Jupiter cannot scatter objects onto these orbits directly after escape from the swarm. Any object that evolved onto an Earth-crossing orbit must first have evolved outward and then been scattered by Saturn.

Asteroids from the main belt could have contributed to and even dominated the LHB, depending on the mass of the belt at the time of the LHB. Migrating planets

caused the ν_6 secular resonance to move from ~ 3.1 AU, depending quite sensitively on the initial locations of the planets, to its current location near 2.1 AU. In our simulations, this migration destabilized 3/4 of the asteroids in this region. Since the timescale of the migration of the ν_6 is tied to the timescale for the migration of the planets themselves, the influx of lunar impactors from this region is related to the migration time of the giant planets. If the asteroid belt contained about the same amount of material at the time of the LHB as it does now, then it would have contributed $< 10\%$ to the LHB. If, on the other hand, it contained approximately an order of magnitude more mass than it does today, it could have contributed most of the impactors.

Although this model appears to explain the LHB very well, there are important caveats that must be noted. This model appears to predict structures for the asteroid belt and Trojan swarms that are inconsistent with observations. However, as explained in §V, the dynamics of these regions are very sensitive to our exact choices of initial placement of the planets. Slightly different initial conditions could alleviate this problems while not affecting our main results (for example, see our run with no migration). In addition, the results for the asteroid belt and Trojans could be due to our simplified model of the physics of these regions.

Perhaps more importantly, this model requires that fully formed Uranus and Neptune not appear in the trans-saturnian region until 700 million years after the formation of the Earth. As described in §III, our understanding of the formation of these planets is at best very sparse, so this requirement is not unreasonable. However, the model presented in this paper must be viewed with some skepticism until formation models of Uranus and Neptune are available that are consistent with this late arrival. Clearly more work needs to be done.

We would like to thank R. Canup, V. Gulick, W. Hartmann, G. Stewart, and W. Ward for useful conversations. We are also grateful to R. Canup and D. Durda

for their comments on an earlier version of the manuscript. We would also like to thank J.-M. Petit and an anonymous referee for comments that significantly strengthened this paper and weakened the authors.

References

- Abe, Y., Drake, M., Okuchi, T., and Righter, K. (2000). Water in the early Earth. In *Origin of the Earth and the Moon* (R. Canup and K. Righter, Eds.), pp. 413–433. Univ. of Arizona Press, Tucson.
- Agnor, C.B., Canup, R.M., and Levison, H.F. (1999). On the character and consequences of large impacts in the late stage of terrestrial planet formation. *Icarus* **142**, 219–237.
- Anbar, A.D., Arnold, G.L., Mojzsis, S.J., and Zahnle, K.J. (2000). Extraterrestrial iridium and sediment accumulation on the Hadean Earth. *J. Geophys. Res.-E*, submitted.
- Arnold, J. R. (1979). Ice in the lunar polar regions. *J. Geophys. Res.* **84**, 5659–5668.
- Baker, V.R., Strom, R.G., Gulick, V.C., Kargel, J., and Komatsu, G. (1991). Ancient oceans, ice sheets and the hydrological cycle on Mars. *Nature* **352**, 589–591.
- Baldwin, R.B. (1949). *The Face of the Moon*. Univ. of Chicago Press, Chicago.
- Baldwin, R.B. (1981). On the origin of the planetesimals that produced the multi-ringed basins. In *Multi-ring Basins, Proc. Lunar Planet. Sci.* 12A (P. Schultz and R.B. Merrill, Eds.), pp. 19-28. Pergamon, New York.
- Baldwin, R.B. (1987a). On the relative and absolute ages of seven lunar front face basins. I - From viscosity arguments. *Icarus* **71**, 1–18.
- Baldwin, R.B. (1987b). On the relative and absolute ages of seven lunar front face basins. II - From crater counts. *Icarus* **71**, 19–29.
- Boss, A.P. (1997). Giant planet formation by gravitational instability. *Science* **276**, 1836–1839.
- Brunini, A., and Fernández, J.A. (1999). Numerical simulations of the accretion of Uranus and Neptune. *Planet. Space Sci.* **47**, 591–605.

- Carlson, R.W., and Lugmair, G.W. (1979). Sm-Nd constraints on early lunar differentiation and the evolution of KREEP. *Earth Planet Sci. Lett.* **45**, 123–132.
- Carlson, R.W., and Lugmair, G.W. (1988). The age of ferroan anorthosite 60025: Oldest crust on a young moon. *Earth Planet. Sci. Lett.* **90**, 119–130.
- Cellino, A., Zappalà, V., and Farinella, P. (1991). The size distribution of main-belt asteroids from IRAS data. *Mon. Not. R. Astron. Soc.* **253**, 561–574.
- Chambers, J.E., and Wetherill, G.W. (1998). Making the terrestrial planets: N-body integrations of planetary embryos in three dimensions. *Icarus* **136**, 304–327.
- Chapman, C.R., and Davis, D.R. (1975). Asteroid collisional evolution - Evidence for a much larger early population. *Science* **190**, 553–556.
- Chapman, C.R. (1976). Chronology of terrestrial planet evolution - The evidence from Mercury. *Icarus* **28**, 523–536 (comments, pp. 537–542).
- Chyba, C.F. (1990). Impact delivery and erosion of planetary oceans in the early inner Solar System. *Nature* **343**, 129–133.
- Chyba, C.F. (1991). Terrestrial mantle siderophiles and the lunar impact record. *Icarus* **92**, 217–233.
- Chyba, C.F., Owen, T.C., and Ip, W.-H. (1994). Impact delivery of volatiles and organic molecules to Earth. In *Hazards Due to Comets and Asteroids* (T. Gehrels and M. S. Matthews, Eds.), pp. 9–58. Univ. of Arizona Press, Tucson.
- Cohen, B.A., Swindle, T.D., and Kring, D.A. (2000). Lunar meteorites support the lunar cataclysm hypothesis. *Science*, **290**, *pages* .
- Culler, T.S., Becker, T.A., Muller, R.A., and Renne, P.R. (2000). Lunar impact history from $^{40}\text{Ar}/^{39}\text{Ar}$ dating of glass spherules. *Science* **287**, 1785–1788.
- Dalrymple, G.B., and Ryder, G. (1993). $^{40}\text{Ar}/^{39}\text{Ar}$ age spectra of Apollo 15 impact

- melt rocks by laser step-heating and their bearing on the history of lunar basin formation. *J. Geophys. Res.* **98**, 13085–13095.
- Delsemme, A.H. (2000). 1999 Kuiper Prize lecture. *Icarus* **146**, 313–325.
- Dones, L., Levison, H.F., Duncan, M.J., and Weissman, P.R. (2000). Formation of the Oort Cloud revisited. *Bull. Amer. Astron. Soc.* **32**, Division for Planetary Sciences meeting abstract 36.02.
- Dones, L., Zahnle, K.J., Bottke, W.F., Jr., and Levison, H.F. (2001). The statistics of large impacts on the terrestrial planets. In preparation.
- Dreibus, G., and Wänke, H. (1989). Supply and loss of volatile constituents during the accretion of terrestrial planets. In *Origin and Evolution of Planetary and Satellite Atmospheres* (S.K. Atreya, J.B. Pollack, and M.S. Matthews, Eds.), pp. 268-288. Univ. of Arizona Press, Tucson.
- Duncan, M., Quinn, T., and Tremaine, S. (1987). The formation and extent of the solar system comet cloud. *Astron. J.* **94**, 1330–1338.
- Feldman, W.C., Maurice, S., Binder, A.B., Barraclough, B.L., Elphic, R.C., and Lawrence, D.J. (1998). Fluxes of fast and epithermal neutrons from Lunar Prospector: Evidence for water ice at the lunar poles. *Science* **281**, 1496–1500.
- Fernández, J.A., and Ip, W.-H. (1984). Some dynamical aspects of the accretion of Uranus and Neptune – The exchange of orbital angular momentum with planetesimals. *Icarus* **58**, 109–120.
- Gladman, B., and Duncan, M. (1990). On the fates of minor bodies in the outer solar system. *Astron. J.* **100**, 1680–1693.
- Gladman, B., Michel, P., and Froeschlé, Ch. (2000). The near-Earth object population. *Icarus* **146**, 176–189.
- Gladman, B., Migliorini, F., Morbidelli, A., Zappalà, V., Michel, P., Cellino, A., Froeschlé, Ch., Levison, H.F., Bailey, M., and Duncan, M. (1997). Dynamical lifetimes of objects injected into asteroid belt resonances. *Science* **277**,

197–201.

- Goldreich, P., and Tremaine, S. (1982). The dynamics of planetary rings. *Ann. Rev. Astron. Astrophys.* **20**, 249–283.
- Gomes, R.S. (1997). Dynamical effects of planetary migration on the primordial asteroid belt. *Astron. J.* **114**, 396–401.
- Gomes, R.S. (1998). Dynamical effects of planetary migration on primordial Trojan-type asteroids. *Astron. J.* **116**, 2590–2597.
- Grinspoon, D.H. (1989) Large impact events and atmospheric evolution on the terrestrial planets. Ph. D. thesis, Univ. of Arizona.
- Guillot, T. (1999). Interiors of giant planets inside and outside the Solar System. *Science* **286**, 72–77.
- Gulick, V.C., Tyler, D., McKay, C.P., and Haberle, R.M. (1997). Episodic ocean-induced CO₂ greenhouse on Mars: Implications for fluvial valley formation. *Icarus* **130**, 68–86.
- Hahn, J.M., and Malhotra, R. (1999). Orbital evolution of planets embedded in a planetesimal disk. *Astron. J.* **117**, 3041–3053.
- Halliday, A.N., Lee, D.-C., and Jacobsen, S.B. (2000). Tungsten isotopes, the timing of metal-silicate fractionation and the origin of the Earth and Moon. In *Origin of the Earth and Moon* (R. Canup and K. Righter, Eds.), pp. 45–62. Univ. of Arizona Press, Tucson.
- Harmon, J.K., Slade, M.A., Vélez, R.A., Crespo, A., Dryer, M.J., and Johnson, J.M. (1994). Radar mapping of Mercury’s polar anomalies. *Nature* **369**, 213–215.
- Hartmann, W.K. (1975). Lunar ‘cataclysm’ - A misconception. *Icarus* **24**, 181–187.
- Hartmann, W.K. (1980). Dropping stones in magma oceans - Effects of early lunar cratering. In *Conference on the Lunar Highlands Crust, Houston, Texas, November 14-16, 1979, Proceedings* (J. Papike and R. Merrill, Eds.), pp. 155-171. Pergamon, New York.

- Hartmann, W.K., Strom, R.G., Grieve, R.A.F., Weidenschilling, S.J., Diaz, J., Blasius, K.R., Chapman, C.R., Woronow, A., Shoemaker, E.M., Dence, M.R., and Jones, K.L. (1981). Chronology of planetary volcanism by comparative studies of planetary cratering. In *Basaltic Volcanism on the Terrestrial Planets*, Basaltic Volcanism Study Project, pp. 1048–1127. Pergamon, New York (full text at <http://adsbit.harvard.edu/books/bvtp/>).
- Hartmann, W.K. (1984). Does crater "saturation equilibrium" occur in the solar system? *Icarus*, **60**, 56–74.
- Hartmann, W.K., Ryder, G., Dones, L., and Grinspoon, D. (2000). The time-dependent intense bombardment of the primordial Earth/Moon system. In *Origin of the Earth and Moon* (R. Canup and K. Righter, Eds.), pp. 493–512. Univ. of Arizona Press, Tucson.
- Haskin, L.A., Korotev, R.L., Rockow, K.M., and Jolliff, B.L. (1998). The case for an Imbrium origin of the Apollo Th-rich impact-melt breccias. *Meteoritics Planet. Sci.* **33**, 959–975.
- Holman, M.J., and Wisdom, J. (1993). Dynamical stability in the outer solar system and the delivery of short period comets. *Astron. J.* **105**, 1987-1999.
- Lecar, M., and Franklin, F. (1997). The solar nebula, secular resonances, gas drag, and the asteroid belt. *Icarus* **129**, 134–146.
- Lecuyer, C., Gillet, Ph., and Robert, F. (1998). The hydrogen isotope composition of sea water and the global water cycle. *Chemical Geology* **145**, 249-261.
- Levison, H.F., and Duncan, M.J. (1994). The long-term dynamical behavior of short-period comets. *Icarus* **108**, 18–36.
- Levison, H., Shoemaker, E.M., and Shoemaker, C.S. (1997). The dispersal of the Trojan asteroid swarm. *Nature* **385**, 42–44.
- Levison, H.F., Lissauer, J.J., and Duncan, M.J. (1998). Modeling the diversity of outer planetary systems. *Astron. J.* **116**, 1998–2014.

- Levison, H., Dones, L., Duncan, M., and Weissman, P. (1999). The formation of the Oort Cloud. *Bull. Amer. Astron. Soc.* **31**, 1079.
- Levison, H.F., Duncan, M.J., Zahnle, K., Holman, M., and Dones, L. (2000). Note: Planetary impact rates from ecliptic comets. *Icarus* **143**, 415–420.
- Liou, J.C., and Malhotra, R. (1997). Depletion of the outer asteroid belt. *Science* **275**, 375–377.
- Lissauer, J.J., Pollack, J.B., Wetherill, G.W., and Stevenson, D.J. (1995). Formation of the Neptune system. In *Neptune* (D.P. Cruikshank, Ed.), pp. 37-108. Univ. of Arizona Press, Tucson.
- Maher, K.A., and Stevenson, D.J. (1988). Impact frustration of the origin of life. *Nature* **331**, 612–614.
- Malhotra, R. (1995). The origin of Pluto’s orbit: Implications for the Solar System beyond Neptune. *Astron. J.* **110**, 420–429.
- Malhotra, R. (1998). Outer planet orbital migration in the early Solar System. *Bull. Amer. Astron. Soc.* **30**, 1389.
- Malhotra, R. (2001). Implications of the Kuiper Belt for the Solar System. *Planet. Space Sci.*, in press.
- Marvin, U.B., Carey, J.W., and Lindstrom, M.M. (1989). Cordierite-spinel troctolite, a new magnesium-rich lithology from the lunar highlands. *Science* **243**, 925–928.
- Marzari, F., Scholl, H., and Farinella, P. (1996). Collision rates and impact velocities in the Trojan asteroid swarms. *Icarus* **119**, 192–201.
- McEwen, A.S., Gaddis, L.R., Neukum, G., Hoffmann, H., Pieters, C.M., and Head, J.W. (1993). Galileo observations of post-Imbrium lunar craters during the first Earth-Moon flyby. *J. Geophys. Res.* **98**, 17207–17234.
- Meier, R., and Owen, T.C. (1999). Cometary deuterium. *Space Science Reviews* **90**, 33–43.

- Melosh, H.J. (1989). *Impact Cratering: A Geologic Process*. Cambridge Univ. Press, New York.
- Mojzsis, S.J., and Ryder, G. (2000). Accretion to Earth and Moon ca. 3.85 Ga. In *Accretion of Extraterrestrial Matter Throughout Earth's History* (B. Schmitz and B. Peucker-Ehrenbrink, Eds.), in press. Kluwer, Norwell, Mass.
- Morbidelli, A., Chambers, J., Lunine, J.I., Petit, J.-M., Robert, F., Valsecchi, G.B., and Cyr, K.E. (2000). Source regions and timescales for delivery of water on Earth. *Meteoritics Planet. Sci.* **35**, 1309–1320.
- Morbidelli, A., Petit, J.-M., Gladman, B., and Chambers, J. (2001). A plausible cause of the Late Heavy Bombardment. *Meteoritics Planet. Sci.* **36**, in press, March 2001.
- Morgan, J.W., Ganapathy, R., Higuchi, H., and Anders, E. (1977). Meteoritic material on the moon. In *The Soviet-American Conference on Cosmochemistry of the Moon and Planets*, Part 2, pp. 659–689 (NASA SP-370).
- Moses, J.I., Rawlins, K., Zahnle, K., and Dones, L. (1999). External sources of water for Mercury's putative ice deposits. *Icarus* **137**, 197–221.
- Murray, C.D. (1986). Structure of the 2:1 and 3:2 Jovian resonances. *Icarus* **65**, 70–82.
- Neukum, G. (1977). Different ages of lunar light plains. *Moon* **17**, 383–393.
- Neukum, G. (1983). *Meteoritenbombardement und Datierung Planetarer Oberflaechen*, Thesis.
- Neukum, G., and Ivanov, B.A. (1994). Crater size distributions and impact probabilities on Earth from lunar, terrestrial-planet, and asteroid cratering data. In *Hazards due to Comets and Asteroids* (T. Gehrels, Ed.), pp. 359–416. Univ. of Arizona Press, Tucson.
- Nozette, S., Lichtenberg, C.L., Spudis, P., Bonner, R., Ort, W., Malaret, E.,

- Robinson, M., and Shoemaker, E.M. (1996). The Clementine bistatic radar experiment. *Science* **274**, 1495–1498.
- Nyquist, L.E., and Shih, C.-Y. (1992). The isotopic record of lunar volcanism. *Geochim. Cosmochim. Acta* **56**, 2213–2234.
- Oberbeck, V.R. and Fogleman, G. (1989). Estimates of the maximum time required to originate life. *Origins of Life* **19**, 549–560.
- Öpik, E.J. (1951). Collision probabilities with the planets and the distribution of interplanetary matter. *Proc. R. Ir. Acad.* **54A**, 165–199.
- Passey, Q.R., Shoemaker, E. M. (1982). Craters and basins on Ganymede and Callisto - Morphological indicators of crustal evolution. In *Satellites of Jupiter* (D. Morrison, Ed.), pp. 379–434. Univ. of Arizona Press, Tucson.
- Pavlov, A.A., Pavlov, A.K., and Kasting, J.F. (1999). Irradiated interplanetary dust particles as a possible solution for the deuterium/hydrogen paradox of Earth's oceans. *J. Geophys. Res. - E* **104**, 30725–30728 (1999).
- Pierazzo, E., and Melosh, H.J. (2000a). Hydrocode modeling of oblique impacts: The fate of the projectile. *Meteoritics Planet. Sci.* **35**, 117–130.
- Pierazzo, E., and Melosh, H.J. (2000b). Understanding oblique impacts from experiments, observations, and modeling. *Ann. Rev. Earth Planet. Sci.* **28**, 141–167.
- Pieters, C.M., Tompkins, S., Head, J.W., and Hess, P.C. (1997). Mineralogy of the mafic anomaly in the South Pole-Aitken Basin: Implications for excavation of the lunar mantle. *Geophys. Res. Lett.* **24**, 1903-1906.
- Pike, R.J. (1982). Morphologic transitions for craters and basins on 13 Solar System bodies. *Lunar Planet. Sci.* **13**, abstract 627–628.
- Pollack, J.B., Kasting, J.F., Richardson, S.M., and Poliakov, K. (1987). The case for a wet, warm climate on early Mars. *Icarus* **71**, 203-224.
- Pollack, J.B., Hubickyj, O., Bodenheimer, P., Lissauer, J.J., Podolak, M., and

- Greenzweig, Y. (1996). Formation of the giant planets by concurrent accretion of solids and gas. *Icarus* **124**, 62–85.
- Righter, K., and Drake, M. (1999). Effect of water on metal-silicate partitioning of siderophile elements: A high pressure and temperature terrestrial magma ocean and core formation. *Earth Planet. Sci. Lett.* **171**, 383–399.
- Ryder, G. (1990). Lunar samples, lunar accretion, and the early bombardment of the Moon. *Eos* **71**, 313, 322–323.
- Ryder, G. (1999). Meteoritic abundances in the ancient lunar crust. *Lunar Planet. Sci.* **30**, #1848 (<http://cass.jsc.nasa.gov/meetings/LPSC99/pdf/1848.pdf>)
- Ryder, G. (2000). The ancient lunar impact record, the ancient terrestrial impact record, and possible environments for the origin of life. Talk at *Catastrophic Events and Mass Extinctions: Impacts and Beyond*, Univ. of Vienna, Vienna, Austria, July 12, 2000 (<http://cass.jsc.nasa.gov/meetings/impact2000/>).
- Ryder, G., Koeberl, C., and Mojzsis, S. (2000). Heavy bombardment of the Earth at ~3.85 Ga: The search for petrographic and geochemical evidence. In *Origin of the Earth and Moon* (R. Canup and K. Righter, eds.), pp. 475–492. Univ. of Arizona Press, Tucson.
- Safronov, V.S. (1972). Ejection of bodies from the Solar System in the course of the accumulation of the giant planets and the formation of the cometary cloud. In *The Motion, Evolution of Orbits, and Origin of Comets*, Proceedings from IAU Symposium #45 (G.A. Chebotarev, E.I. Kazimirchak-Polonskaia, and B.G. Marsden, Eds.), p. 329. Reidel, Dordrecht.
- Schenk, P.M., and Moore, J.M. (1999). On the Importance of Being Lofn: Geology of Large Impact Basins on Callisto *Lunar Planet. Sci.* **30**, #1786
- Shoemaker, E.M., and Wolfe, R.F. (1984). Evolution of the Uranus-Neptune planetesimal swarm. *Lunar Planet. Sci.* **15**, 780–781.
- Simpson, R.A., and Tyler, G.L. (1999). Reanalysis of Clementine bistatic radar

- data from the lunar South Pole. *J. Geophys. Res.* **104**, 3845–3862.
- Slade, M.A., Butler, B.J., and Muhleman, D.O. (1992). Mercury radar imaging - Evidence for polar ice. *Science* **258**, 635–640.
- Sleep, N.H., Zahnle, K.J., Kasting, J.F., and Morowitz, H.J. (1989). Annihilation of ecosystems by large asteroid impacts on the early Earth. *Nature* **342**, 139–142.
- Smith, D.E., Zuber, M.T., Neumann, G.A., and Lemoine, F.G. (1997). Topography of the Moon from the Clementine lidar. *J. Geophys. Res.* **102**, 1591–1611.
- Stacy, N.J.S., Campbell, D.B., and Ford, P.G. (1997). Arecibo radar mapping of the lunar poles: A search for ice deposits. *Science* **276**, 1527–1530.
- Stern, S.A., and Levison, H.F. (1999). A warm early Mars and CO₂ influx from the Late Heavy Bombardment. *Lunar Planet. Sci.* **30**, abstract #1141 (<http://cass.jsc.nasa.gov/meetings/LPSC99/pdf/1141.pdf>).
- Stern, S.A., and Weissman, P.R. (2000). Cometary collisional evolution during ejection to the Oort cloud. *Nature*, submitted.
- Stern, S.A., Slater, D.C., Festou, M.C., Parker, J.W., Gladstone, G.R., A’Hearn, M.F., and Wilkinson, E. (2001) The discovery of argon in comet C/1995 O1 (Hale-Bopp) *Astrophys. J. Lett.* **544**, L169–L172.
- Stewart, G.R., and Levison, H.F. (1998). On the formation of Uranus and Neptune. *Lunar Planet. Sci.* **29**, #1960 (<http://cass.jsc.nasa.gov/meetings/LPSC98/pdf/1960.pdf>).
- Strom, R.G., and Neukum, G. (1988). The cratering record on Mercury and the origin of impacting objects. In *Mercury* (F. Vilas, C.R. Chapman, and M.S. Mathews, eds.), pp. 336–373. Univ. of Arizona Press, Tucson.
- Swindle, T.D. & Kring, D.A. (2001) Cataclysm + cold comets = lots of asteroid impacts. *Lunar Planet. Sci.* **32**, in press.
- Taylor, S.R. (1982). *Planetary Science: A Lunar Perspective*. Lunar and Planetary Science Institute, Houston.

- Tera, F., Papanastassiou, D.A., and Wasserburg, G.J. (1974). Isotopic evidence for a terminal lunar cataclysm. *Earth Planet. Sci. Lett.* **22**, 1–21.
- Thommes, E.W., Duncan, M.J., and Levison, H.F. (1999). The formation of Uranus and Neptune in the Jupiter-Saturn region of the Solar System. *Nature* **402**, 635–638.
- Tremaine, S., and Dones, L. (1993). On the statistical distribution of massive impactors. *Icarus* **106**, 335–341.
- Trujillo, C.A., Jewitt, D.C., and Luu, J.X. (2000). Population of the scattered Kuiper Belt. *Astrophys. J.* **529**, L103–L106.
- Vasavada, A.R., Paige, D.A., and Wood, S.E. (1999). Near-surface temperatures on Mercury and the Moon and the stability of polar ice deposits. *Icarus* **141**, 179–193.
- Walker, J.C.G. (1977). *Evolution of the Atmosphere*, Macmillan, New York.
- Ward, W.R. (1975). Past orientation of the lunar spin axis. *Science* **189**, 377–379.
- Ward, W.R. (1980). Scanning secular resonances: A cosmogonical broom? *Lunar Planet. Sci.* **11**, 1199–1201.
- Ward, W.R., and Hahn, J.M. (1998a). Neptune’s eccentricity and the nature of the Kuiper Belt. *Science*, **280**, 2104–2106.
- Ward, W.R., and Hahn, J.M. (1998b). Dynamics of the trans-Neptune region: Apsidal waves in the Kuiper Belt. *Astron. J.* **116**, 489–498.
- Weidenschilling, S.J. (1977). The distribution of mass in the planetary system and solar nebula. *Astrophys. Space Sci.* **51**, 153–158.
- Weissman, P.R. (1996). The Oort cloud. In *Completing the Inventory of the Solar System* (T.W. Rettig and J.M. Hahn, Eds.) pp. 265–288. Astronomical Society of the Pacific, San Francisco.
- Wetherill, G.W. (1975). Late heavy bombardment of the moon and terrestrial planets. In *Lunar Science Conference, 6th, Proceedings*, Volume 2,

- pp. 1539-1561. Pergamon, New York.
- Wetherill, G.W. (1981). Nature and origin of basin-forming projectiles. In *Multi-Ring Basins: Formation and Evolution*, pp. 1-18. Pergamon, New York.
- Wetherill, G.W., Allègre, C.J., Brooks, C., Eberhardt, P., Hart, S.R., Murthy, V.R., Tera, F., and van Schmus, W.R. (1981). Radiogenic and stable isotopes, radiometric chronology, and basaltic volcanism. In *Basaltic Volcanism on the Terrestrial Planets*, Basaltic Volcanism Study Project, pp. 901-1047. Pergamon, New York (full text at <http://adsbit.harvard.edu/books/bvtp/>).
- Wieczorek, M.A., and Phillips, R.J. (1998). Potential anomalies on a sphere – Applications to the thickness of the lunar crust. *J. Geophys. Res.* **103**, 1715-1724.
- Wieczorek, M.A., and Phillips, R.J. (1999). Lunar multiring basins and the cratering process. *Icarus* **139**, 246-259.
- Wilhelms, D.E. (1987) *The Geologic History of the Moon*. U.S. Geol. Surv. Prof. Pap. 1348, 302 pp.
- Wisdom, J. (1980). The resonance overlap criterion and the onset of stochastic behavior in the restricted three-body problem. *Astron. J.* **85**, 1122-1133.
- Wisdom, J. (1983). Chaotic behavior and the origin of the 3/1 Kirkwood gap. *Icarus* **56**, 51-74.
- Wisdom, J., and Holman, M. (1991). Symplectic maps for the n-body problem. *Astron. J.* **102**, 1528-1538.
- Zahnle, K. (1998). Origins of atmospheres. In *Origins*, ASP Conference Series, Vol. 148 (Charles E. Woodward, J. Michael Shull, and Harley A. Thronson, Jr., Eds.), pp. 364-391. Astronomical Society of the Pacific, San Francisco.
- Zahnle, K.J., and Sleep, N.H. (1997). Impacts and the early evolution of life. In *Comets and the Origin and Evolution of Life* (P.J. Thomas, C.F. Chyba, and

C.P. McKay, Eds.), pp. 175-208. Springer-Verlag, New York.

Zappalà, V., Cellino, A., Gladman, B.J., Manley, S., and Migliorini, F. (1998)
Asteroid showers on Earth after family break-up events. *Icarus* **134**, 176–179.

Figure Captions

Figure 1 — The temporal evolution of Jupiter’s semi-major axis during our main simulations. In these simulations, a fictitious force is applied to the giant planets in order to mimic the migration that occurs due to the planets gravitationally scattering a large number of small bodies. See text for details. This force decreases exponentially with a time constant, τ . A) $\tau = 10^7$ years. B) $\tau = 3 \times 10^7$ years.

Figure 2 — The dynamical lifetimes for objects in the asteroid belt for two different models of the planetary system. The integrations used to estimate these lifetimes lasted for 10^8 years (shown as dotted lines in the figures). Thus, any particle shown to have a lifetime of 10^8 years was stable in the simulation and has a real dynamical lifetime that is greater than this. The locations of the 3:1 and 2:1 mean motion resonances with Jupiter, as well as the ν_6 secular resonance, are shown in the figures. A) The dynamical lifetime of main belt asteroids in the pre-migrated Solar System. B) The dynamical lifetime of main belt asteroids in the current Solar System.

Figure 3 — The normalized impact history of the Moon from Uranus-Neptune planetesimals as predicted from our simulations. The height of each bar indicates the fraction of objects that impacted the Moon over a time period of 2 million years. The origin of the plot is taken to be the time of Uranus and Neptune’s formation. A) $\tau = 10^7$ year run. B) $\tau = 3 \times 10^7$ year run. C) The no migration run.

Figure 4 — The impact rate per unit area on each of the terrestrial planets relative to that on the Moon as predicted by Öpik’s equations. The numbers presented were calculated by dividing the total number of impacts by the

planet’s surface area. Thus, these numbers do not include any differences in crater densities that would arise from differences in impact velocities or sizes of impactors. The red, blue, and brown show results from our $\tau = 10^7$ year, $\tau = 3 \times 10^7$ year, and no migration (‘nm’) runs, respectively. A) Impacts due to Uranus-Neptune planetesimals. (Note that there were no impacts on Mercury in the $\tau = 3 \times 10^7$ year run.) B) Impacts due to Jovian Trojans. C) Impacts due to asteroids from the main belt.

Figure 5 — A) The probability that an encounter with Jupiter will lead to an orbit that crosses the orbit of one of the terrestrial planets as a function of dimensionless encounter velocity, U . The top axis shows the Tisserand parameter, T . Curves for Venus, Earth, and Mars are shown. B) The cumulative distribution of U of objects originally between Uranus and Neptune as they cross the orbit of Jupiter. The solid curve is data taken from our $\tau = 10^7$ year run from the Uranus-Neptune region. The dashed curve is from the Trojan, $\tau = 10^7$ year run.

Figure 6 — Same as Figure 3, except for escaped Trojans.

Figure 7 — Same as Figure 3, except for asteroids from the main belt. Note that the horizontal scale is different from Figures 3 and 6.

Figure 8 — The dynamical lifetimes for objects in the asteroid belt for our $\tau = 10^7$ year run. The integration lasted for 10^8 years (shown as dotted lines in the figure). Thus, any particle shown to have a lifetime of 10^8 years was stable in the simulation and has a real dynamical lifetime that is greater than this. The migration of the 3:1 and 2:1 mean motion resonances with Jupiter, as well as the ν_6 secular resonance, are shown in the figure as arrows. In all cases the resonances move from right to left in the figure.

FIGURE 1

Jupiter's Semi-major Axis

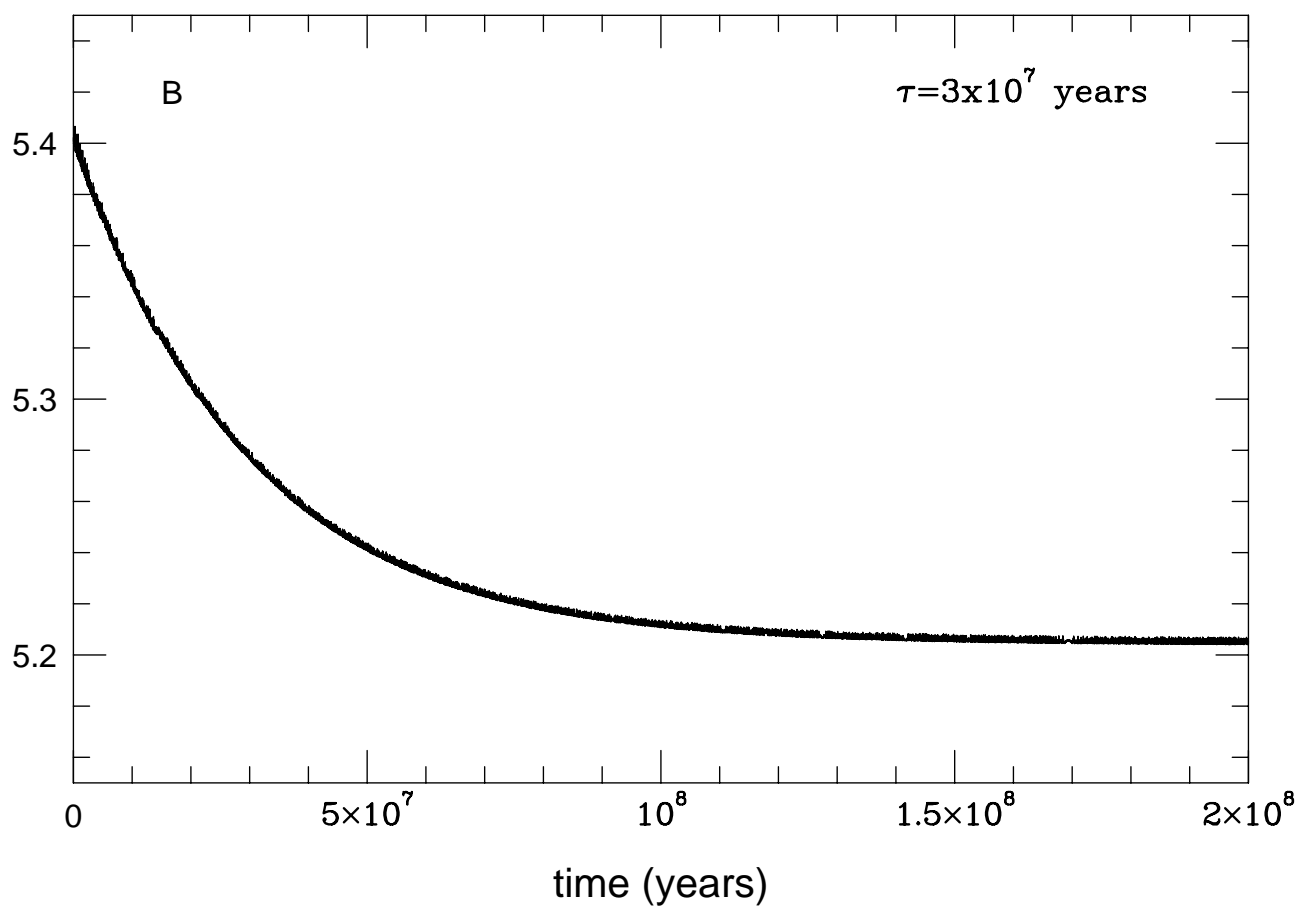
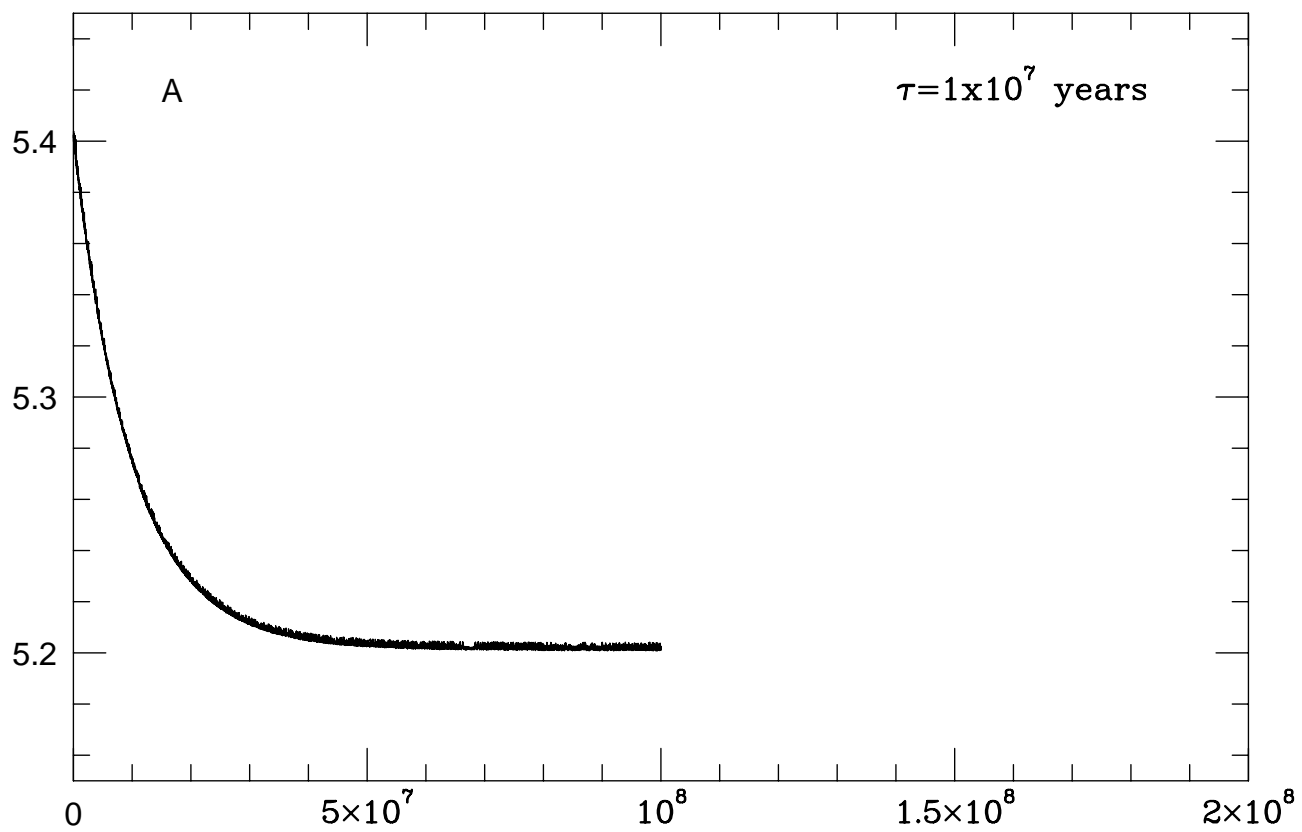


FIGURE 2

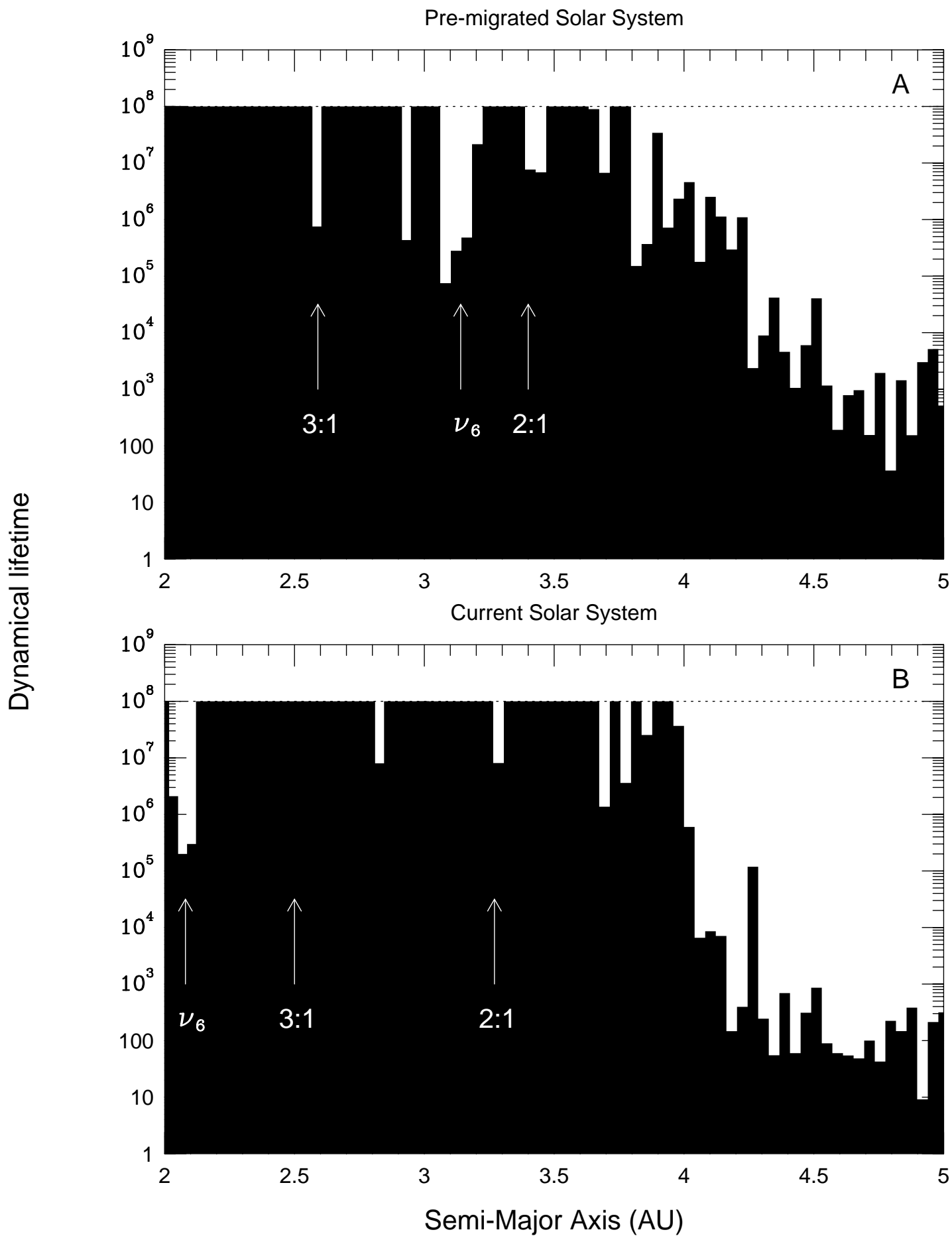


FIGURE 3

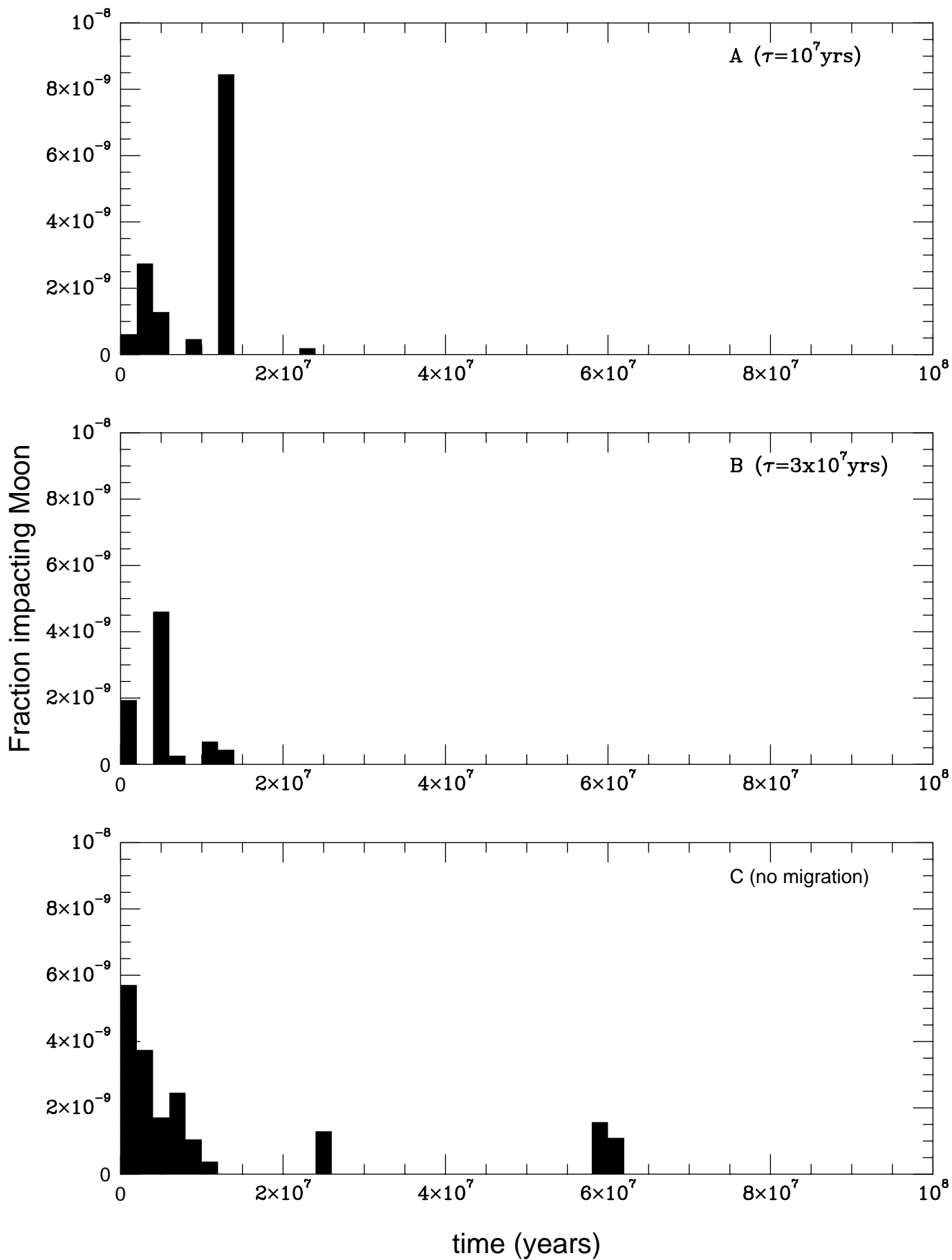


FIGURE 4

Impact Rate Per Unit Area Relative to Moon

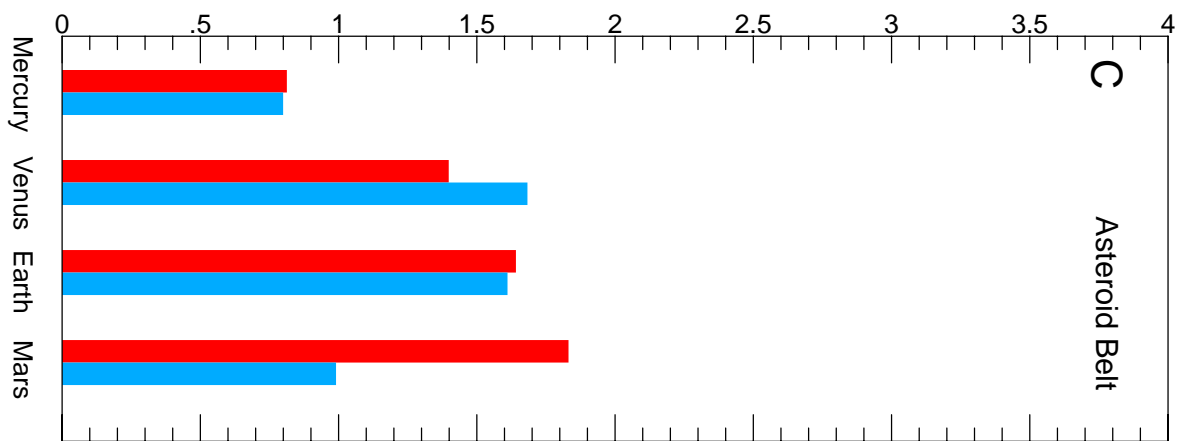
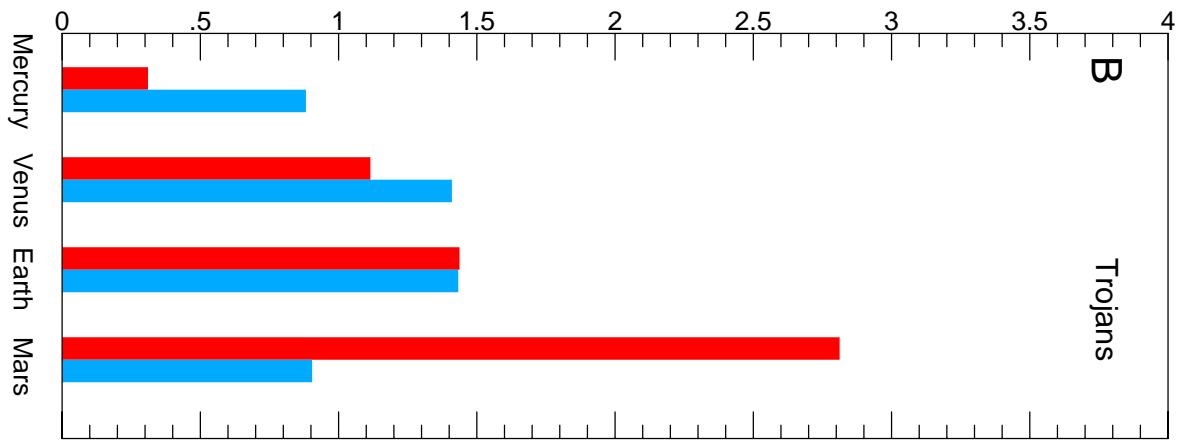
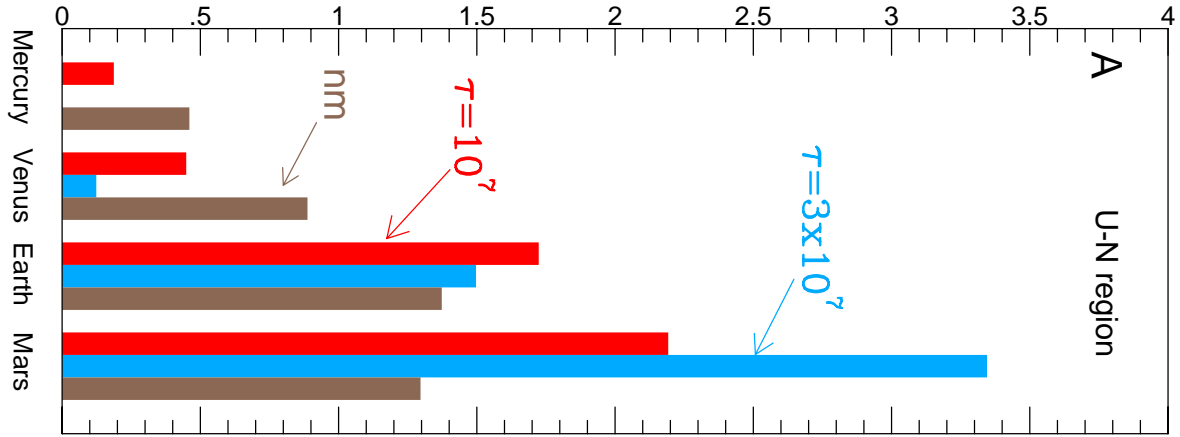


FIGURE 5

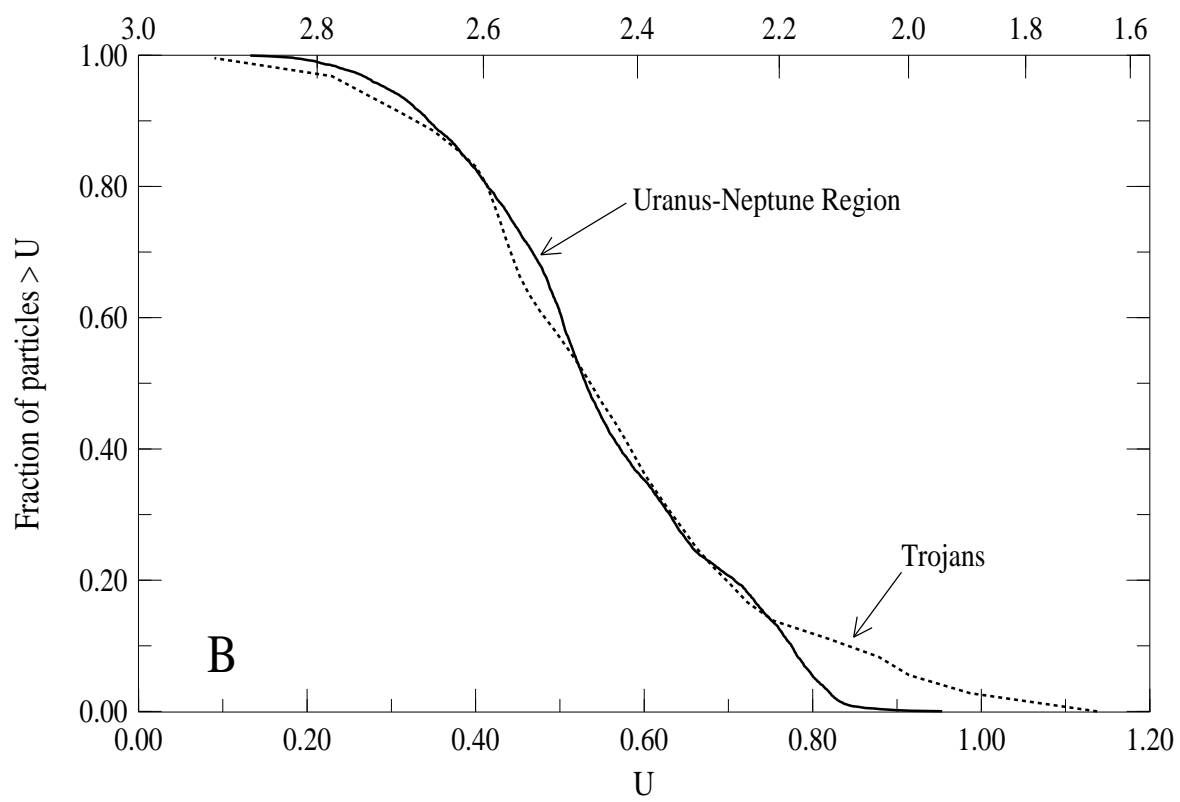
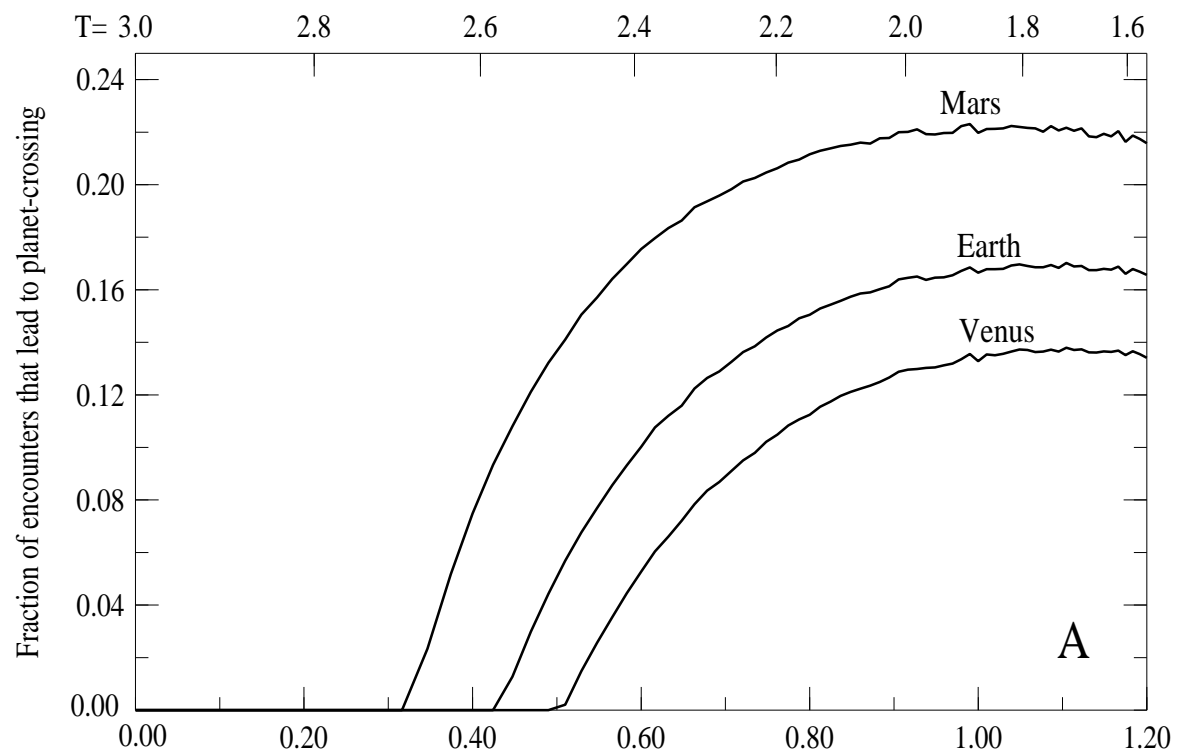


FIGURE 7

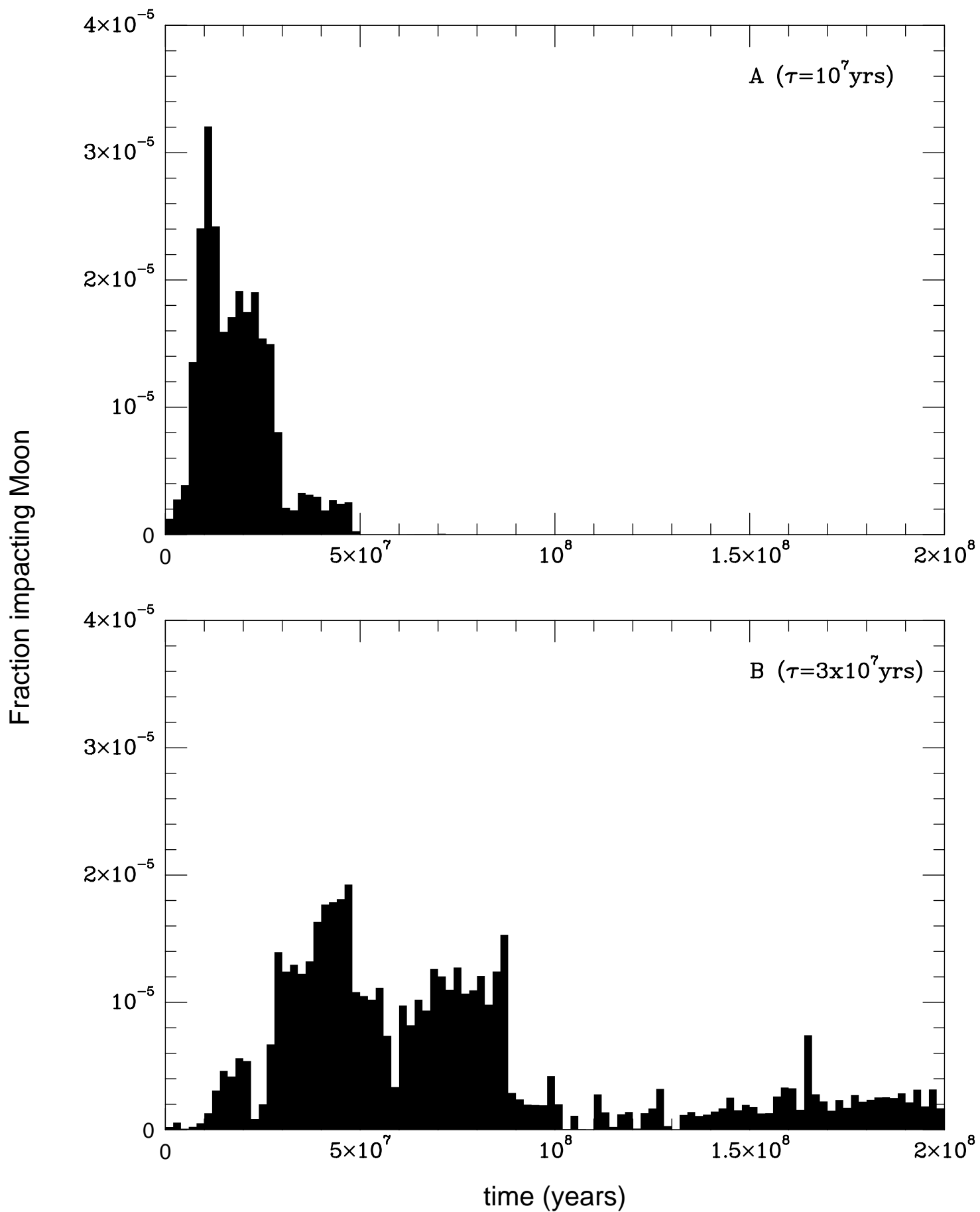


FIGURE 8

